Group B Streptococcus Degrades Cyclic-di-AMP to Modulate STING-Dependent Type I Interferon Production.

Warrison A Andrade, Arnaud Firon, Tobias Schmidt, Veit Hornung, Katherine A Fitzgerald, Evelyn A Kurt-Jones, Patrick Trieu-Cuot, Douglas T Golenbock, Pierre-Alexandre Kaminski

HAL Id: pasteur-01483976
https://pasteur.hal.science/pasteur-01483976

Submitted on 6 Mar 2017

Group B *Streptococcus* degrades cyclic-di-AMP to

modulate STING-dependent type I interferon production

Warrison A. Andrade[1, 2, 6], Arnaud Firon[3, 4, 6], Tobias Schmidt[5], Veit Hornung[5], Katherine A. Fitzgerald[1, 2], Evelyn A. Kurt-Jones[1, 2], Patrick Trieu-Cuot[3, 4*], Douglas T. Golenbock[1, 2, 7*], and Pierre-Alexandre Kaminski[3, 4, 7]

[1]Division of Infectious Diseases and Immunology and [2]Program in Innate Immunity, Department of Medicine, University of Massachusetts Medical School, Worcester, MA 01605, USA

[3]Institut Pasteur, Unité de Biologie des Bactéries Pathogènes à Gram-Positif, [4]Centre National de la Recherche Scientifique (CNRS) ERL 3526, 75724 Paris, France

[5]Institute of Molecular Medicine, Universitätsklinikum Bonn, Bonn, 53127, Germany.

[6]Co-first author

[7]Co-senior author

*Co-corresponding authors

Keywords: Interferon-ß, *Streptococcus agalactiae*, cGAS, c-di-AMP, ectonucleotidase

Please address correspondence to Douglas T. Golenbock, Department of Medicine, University of Massachusetts Medical School, 364 Plantation St., Worcester, MA 01605. Phone: 508 856 5982; FAX: 508 856 8447. Email: douglas.golenbock@umassmed.edu and Patrick Trieu-Cuot, Unite de Biologie des Bacteries Pathogenes a Gram-Positif, Institut Pasteur, 25 rue du Dr. Roux, 75724 Paris, France. Phone: 33 1 44 38 95 92. Fax: 33 1 45 68 89 38. E-mail: patrick.trieu-cuot@pasteur.fr

Running Title: GBS ectonucleotidase controls type I interferon production

SUMMARY

Induction of type I interferon in response to microbial pathogens depends on a conserved cGAS-STING signaling pathway. The presence of DNA in the cytoplasm activates cGAS, while STING is activated by cyclic dinucleotides (cdNs) produced by cGAS or from bacterial origins. Here, we show that Group B *Streptococcus* (GBS) induces IFN-ß production almost exclusively by a cGAS-STING-dependent recognition of bacterial DNA. However, we found that GBS expressed an ectonucleotidase, CdnP, which hydrolyzes extracellular bacterial cdN. Inactivation of CdnP leads to c-di-AMP accumulation outside the bacteria and increased IFN-ß production *in vitro* and *in vivo*. Higher IFN-ß levels *in vivo* increased GBS killing by the host. The IFN-ß overproduction observed in the absence of CdnP is due to the cumulative effect of DNA sensing by cGAS and STING-dependent sensing of c-di-AMP. Our findings uncover the first c-di-AMP ectonucleotidase and suggest a direct bacterial mechanism dampening the activation of the cGAS-STING axis.

INTRODUCTION

Type I interferon (IFN) production is a conserved pro-inflammatory response to microbial infections (McNab et al., 2015). However, the production of type I IFN can be beneficial or detrimental to the host in the case of bacterial infections (Monroe et al., 2010). For instance, the type I IFN response is detrimental for the host during infections by *Listeria monocytogenes*, *Mycobacterium tuberculosis* and *Neisseria gonorrhoeae* (Archer et al., 2014; Manzanillo et al., 2012). In contrast, type I IFN is critical for host defenses against certain extracellular pathogens such as *Streptococcus* species (e.g., *S. pneumoniae*, *S. pyogenes*, *S. agalactiae*) and *Staphylococcus aureus* (Gratz et al., 2011; Mancuso et al., 2007; Parker et al., 2014). Induction of type I IFN in response to bacteria is dependent on two main pathways (Monroe et al., 2010). The first pathway is a Toll-like receptor 4 (TLR4)-dependent sensing of LPS molecules present on the surface of gram-negative bacteria. The second pathway is a cytosolic sensing of bacterial nucleic acids, mainly double-stranded DNA, present in the host cytoplasm.

Several cytoplasmic DNA receptors have been identified, among which the recently described cyclic GMP-AMP synthase (cGAS) has a critical role (Barber, 2014; Cai et al., 2014; Paludan, 2015). The cGAS enzyme is activated by DNA binding and produces a specific eukaryotic cyclic dinucleotide (cdN), abbreviated hereafter as 2'3' cGAMP (Ablasser et al., 2013; Gao et al., 2013a) which acts as a second messenger to activate the endoplasmic reticulum (ER)-localized protein stimulator of IFN genes (STING). Once activated, STING recruits TANK-Binding Kinase 1 (TBK1) to phosphorylate interferon regulatory factor 3 (IRF3), ultimately leading to type I IFN production.

Prior to the discovery of 2'3' cGAMP, only bacteria were known to synthesize cdNs. All bacteria synthesize at least one cdN, either c-di-AMP, c-di-GMP, and/or cGAMP, which acts as a secondary messenger in several processes such as biofilm formation, cell wall homeostasis,

3

bacterial growth, or virulence gene expression (Corrigan and Grundling, 2013; Romling et al., 2013). In addition to their intracellular functions for bacterial physiology, cdNs are secreted or released outside bacteria and recognized by the innate immune system (Danilchanka and Mekalanos, 2013). Cytosolic sensing of bacterial cdN induces IFN-ß production through activation of STING (Burdette et al., 2011; McWhirter et al., 2009; Woodward et al., 2010).

Given the overlapping induction by DNA through the cGAS-STING axis and by bacterial cdN through STING activation, the main bacterial inducer of the IFN-ß response remains to be identified (Danilchanka and Mekalanos, 2013). On one hand, STING-dependent induction of IFN-ß correlates with the amount of secreted bacterial cdN (Barker et al., 2013; Dey et al., 2015; Schwartz et al., 2012; Woodward et al., 2010; Yamamoto et al., 2012). On the other hand, the affinity of STING for bacterial cdN is lower compared to 2'3' cGAMP (Gao et al., 2013b; Kranzusch et al., 2015; Zhang et al., 2013). The relative contribution of DNA and bacterial cdN sensing for IFN-ß induction have been recently evaluated using cGAS- and STING-deficient cells infected with the intracellular pathogens *M. tuberculosis*, *L. monocytogenes* and *Chlamydia trachomatis*. Overall, bacterial DNA recognition by cGAS seems to be the main stimulus for IFN-ß induction and the role of bacterial cdN remains controversial. Some studies suggest that bacterial cdN does not play a significant role in IFN-ß induction (Collins et al., 2015; Hansen et al., 2014; Wassermann et al., 2015; Watson et al., 2015; Zhang et al., 2014), while others indicate the opposite or a species-dependent role (Barker et al., 2013; Dey et al., 2015; Schwartz et al., 2012; Woodward et al., 2010; Yamamoto et al., 2012).

In this study, we characterized the IFN-ß response to *S. agalactiae* (the Group B *Streptococcus*, GBS), a commensal bacteria of the human intestinal and vaginal flora, but the leading cause of neonatal invasive infections in developed countries (Joubrel et al., 2015). We previously demonstrated that GBS induces IFN-ß by a TBK1-IRF3-dependent and TLR-

independent pathway in murine macrophages in response to live bacteria (Charrel-Dennis et al., 2008). Here we report that GBS induces type I IFN by a cGAS- and STING-dependent pathway, primarily upon recognition of bacterial DNA, in murine macrophages and human monocytes. However, we observed that GBS degrades c-di-AMP present outside the bacteria. We showed that c-di-AMP is produced by GBS, but the amount of extracellular c-di-AMP is kept low by the activity of the cell wall-anchored ectonucleotidase CdnP. The CdnP enzyme is unrelated to the currently known bacterial cdN phosphodiesterases and acts sequentially with a second ectonucleotidase, NudP (Firon et al., 2014), to degrade extracellular c-di-AMP into adenosine. We show that inactivation of CdnP leads to c-di-AMP accumulation outside the bacteria and an overproduction of IFN-ß due to a STING-dependent, cGAS-independent, recognition of c-di-AMP. We thus report a novel and direct mechanism used by a bacteria to dampen IFN-ß production by degrading c-di-AMP to prevent STING overactivation.

RESULTS

cGAS is the main sensor for IFN induction in response to WT GBS.

We previously demonstrated that type I IFN production in response to GBS relies on GBS phagocytosis, alteration of the phagolysosomal membrane by the bacterial pore-forming toxin ß-hemolysin/cytolysin, and the release of bacterial DNA into the cytosol (Charrel-Dennis et al., 2008). To clarify the role of the DNA sensors cGAS and the DNA-binding PYHIN family member, IFI16, in GBS infection, human THP-1 cells were infected with GBS bacteria. We observed robust IFN-ß induction by WT GBS infection in THP-1 cells (Figure 1A) consistent with our previous results in murine bone marrow-derived macrophages (BMDMs) (Charrel-Dennis et al., 2008). Using cGAS$^{-/-}$ or IFI16$^{-/-}$ THP-1 cell lines, we demonstrate that IFN-ß induction by WT GBS depends mostly, but not exclusively, on cGAS (Figure 1A), and is

independent of IFI16 (Figure 1B). In agreement with cGAS acting upstream of the adapter STING, we observed a similar drop in IFN-ß induction by WT GBS in STING^{-/-} THP-1 cells (Figure 1C). The level of IFN-ß induction observed at the mRNA level was confirmed by the quantification of IP-10, a surrogate cytokine for type I IFN expression, in WT, cGAS^{-/-}, and STING^{-/-} THP-1 cells (Figures 1D and 1E). Transfection of purified GBS DNA confirmed the critical function of the cGAS-STING axis for IFN-ß production in response to cytoplasmic DNA (Figures 1A-E). Moreover, infections with GBS lacking cytolysin ($\Delta cylE$) confirmed the important function of this toxin for type I IFN induction (Figures 1A-E).

Similar results were obtained with murine BMDMs. Induction of IFN-ß in BMDMs infected with GBS is strongly and similarly decrease in cGAS^{-/-} and STING^{-/-} cells (Figures 1F and 1G). The cGAS-STING axis has only a slight effect on TNF-α expression (Figures 1F and 1G) demonstrating the conserved and specific role of the cGAS-STING axis in response to GBS infection. Overall, we confirmed our previous study describing that WT GBS induces type I IFN by a DNA-dependent sensing pathway, and identified cGAS as the main upstream component mediating this response. In addition, the similar response observed in cGAS^{-/-} and STING^{-/-} cells was consistent with cGAS relaying the information to STING through the synthesis of 2'3' cGAMP and suggests that activation of STING directly by GBS cdN, independently of cGAS, plays a minor role.

GBS hydrolyzes extracellular c-di-AMP

To understand the putative role of bacterial cdN in IFN-ß induction by WT GBS, we looked for genes involved in cdN synthesis in the GBS genome. Homologues of the DacA di-adenylate cyclase (Gbs0902) and of the GdpP intracellular c-di-AMP phosphodiesterase (Gbs2100), the two conserved enzymes involved in c-di-AMP synthesis and intracellular degradation (Corrigan and Grundling, 2013) were identified, in contrast to genes encoding enzymes involved in c-di-GMP

and cGAMP metabolism (Davies et al., 2012; Romling et al., 2013). Consistently, c-di-AMP, but not c-di-GMP or cGAMP, was detected in GBS extracts (Figure 2A).

Cyclic-di-AMP is released outside bacteria by a mechanism involving non-specific transporters (Kaplan Zeevi et al., 2013; Woodward et al., 2010; Yamamoto et al., 2012), and could also occur through spontaneous lysis (Oliveira et al., 2012). However, the absence of STING activation independent of cGAS suggests a low level of c-di-AMP outside GBS. We therefore hypothesized that GBS may degrade extracellular c-di-AMP. To test this hypothesis, intact WT GBS cells were incubated with exogenously added c-di-AMP. In this condition, the concentration of extracellular c-di-AMP decreases linearly (Figure 2B) coinciding with an accumulation of extracellular adenosine (Figure 2C).

The formation of adenosine suggests the involvement of the NudP ectonucleotidase that degrades extracellular ADP and AMP into adenosine (Firon et al., 2014). Interestingly, the rate of c-di-AMP hydrolysis is slower with Δ*nudP* mutant cells compared to WT bacteria (Figure 2B) and AMP production is observed instead of adenosine formation (Figure 2C). Overall, these results demonstrate that GBS hydrolyzes extracellular c-di-AMP and suggest that an enzyme present at the bacterial surface hydrolyzes extracellular c-di-AMP into AMP, which is further processed into adenosine by NudP.

The ectonucleotidase CdnP degrades extracellular c-di-AMP

Among the approximately 30 GBS proteins with a cell wall anchoring motif (Glaser et al., 2002), we identified a second ectonucleotidase Gbs1929 (NCBI WP_000033934.1), hereafter named CdnP for cyclic dinucleotide phosphodiesterase. CdnP is an 800-aa protein containing a signal peptide, a canonical LPxTG cell surface localization motif, a 5'-nucleotidase domain, and a metallophosphoesterase domain (Figure 2D). CdnP has a conserved NHE motif (residues 198-200) in which the histidyl residue is essential for metallophosphodiesterase activity (Matange et

7

al., 2015; Zimmermann et al., 2012). Therefore, we engineered the GBS chromosome to replace the His$_{199}$ residue with an alanine (Figure 2D). The resulting inactivated CdnP mutant (Δ*cdnp**) is unable to hydrolyze exogenously added c-di-AMP (Figures 2B and 2C). This result indicates that CdnP is indeed the enzyme responsible for c-di-AMP extracellular degradation by GBS.

To further demonstrate that c-di-AMP is released extracellularly by GBS, we analyzed WT and Δ*cdnp** supernatants by HPLC. Almost no c-di-AMP was detected in the WT GBS supernatant, in contrast to the Δ*cdnp** supernatant (Figure S2A). To compare the amount of extracellular c-di-AMP, we adapted a c-di-AMP quantification assay based on the *S. pneumoniae* c-di-AMP binding protein CabP (Bai et al., 2014). Resin-bound CabP was used to bind c-di-AMP present in GBS supernatants and bound nucleotides were quantitated by HPLC after elution (Figure S2B). Supernatants of WT and WTbk control (the WT CdnP strain isogenic to Δ*cdnP**) contain a similar low amount of extracellular c-di-AMP. In contrast, the Δ*cdnP** supernatant contains 5- to 7-fold more extracellular c-di-AMP (Figure 2E). These results strongly suggest that the low level of extracellular c-di-AMP observed in WT supernatants is due to the CdnP activity.

CdnP has 2',3' cNMP activity

CdnP is annotated as a putative bifunctional 2',3'-cyclic-nucleotide 2'-phosphodiesterase and 3'-nucleotidase (EC 3.1.4.16) based on homology with CpdB from *Escherichia coli*. CpdB-related proteins are predicted to hydrolyze the cyclic phosphoester linkage of 2',3' cyclic nucleotides (2',3' cNMP) to give 2' or 3' monophosphate nucleotides (2' NMP or 3' NMP), among which the 3' NMP can be further hydrolyzed by the same enzyme to give the corresponding nucleoside and inorganic phosphate (Anraku, 1964).

To characterize the enzymatic activity, we purified the recombinant rCdnP (Figure 2D: residues 28-798). The rCdnP protein is soluble and has an apparent molecular mass of about 80 kDa, in agreement with its theoretical 82 kDa mass. Sedimentation velocity experiments revealed

an $s_{20,w}$ of 4.2 S and a frictional ratio of 1.6, giving a calculated mass of 80 kDa, corresponding to a monomeric protein displaying an elongated shape (Figure 3A). Purified rCdnP converts the predicted substrate 2',3' cNMP to nucleoside and phosphate (Figure S3A). The optimal enzymatic activity is at pH 7.5 (Figure 3B) and is dependent on manganese with an optimum near 0.5 mM (Figure 3C). There is a stringent Mn^{2+} requirement since only low activity was observed with Ca^{2+} and no activity was detected with other divalent ions such as Mg^{2+}, Co^{2+}, or Zn^{2+} (Figure 3C). The substrate specificity and kinetic parameters of rCdnP were determined in the presence of 2 mM Mn^{2+} at pH 7.5. The Michaelis constants of rCdnP are shown in Table 1 and the highest specific activity was obtained with 2',3' cUMP (Figure S3A). In contrast, CdnP has no activity on 3',5' cNMP, including the universal second messenger cAMP (Table 1 and Figure S3A). Since 2',3' cNMPs are instable *in vivo* (Rao et al., 2010), we hypothesized that they are not the CdnP physiological substrates.

CdnP is a 3'5' cyclic dinucleotide 3' phosphodiesterase

Based on our observation with intact GBS cells, we further characterized the substrate specificity of CdnP. Remarkably, bacterial cdNs were hydrolyzed by rCdnP to give the corresponding 5' NMP nucleotides (Figures 3D and 3E). We determined the Michaelis constants for c-di-AMP, c-di-GMP, and cGAMP (Table 1) and observed the highest specific activity (7 μmol P_i/ min/ mg prot) with c-di-AMP (Figure S3B). In agreement with the data obtained with GBS cells, we observed that CdnP and NudP cooperate to cleave c-di-AMP into adenosine. CdnP cleaves the two 3' phosphodiester bonds of c-di-AMP to give two 5' AMP molecules, which are further cleaved by NudP to give two adenosine and two inorganic phosphates (Figure S3B).

Bacterial cdNs are made of two 3',5' phosphodiester linkages connecting the base units. In contrast, the metazoan 2'3' cGAMP (>G(2',5')pA(3',5')p>) contains one 2',5' and one 3',5' phosphodiester linkage (Ablasser et al., 2013; Gao et al., 2013a). While CdnP hydrolyzes the

bacterial cGAMP containing two 3',5' linkages, no activity was detected on the metazoan 2'3' cGAMP (Table 1 and Figure S3B). Interestingly, addition of 2'3' cGAMP does not inhibit the activity of rCdnP on the other substrates (data not shown). On the other hand, non-hydrolysable c-di-NMP analogs, such as cyclic diadenosine monophosphorodithioate, Rp-isomers (Rp, Rp-c-diAMPSS), a di-thiophosphate analogue of c-di-AMP, inhibit rCdnP activity (Figure S3C). In addition, modifications of the 2', 2'' positions of the ribose, by adding fluor or O-methyl-ribose, influence the catalytic efficiency of rCdnP (data not shown). It is thus likely that the metazoan 2'3' cGAMP is not a substrate for rCdnP because the specific conformation imposed by the 2',5' linkage may hinder the substrate-enzyme interaction (Collins et al., 2015).

To confirm the enzymatic activity, we purified the recombinant rCdnP* where the CdnP critical His_{199} residue was mutated to Ala. In similar conditions, rCdnP* was totally inactive whatever the substrate used (Figure 3E and data not shown). These results demonstrate that CdnP is a 3',5' cyclic dinucleotide 3' phosphodiesterase.

Degradation of c-di-AMP by CdnP limits STING activation

IFN-ß induction in response to GBS appears mainly dependent on DNA recognition by cGAS while the direct activation of STING by c-di-AMP has at best a minor role when using WT bacteria (Figure 1). However, WT GBS degrades c-di-AMP present outside the bacteria due to the CdnP ectonucleotidase (Figures 2 and 3). To uncover the effect of CdnP, we compared IFN-ß induction in THP-1 cells infected with WT GBS, Δ*cdnP** mutant, or the isogenic WTbk control. At all MOIs tested, transcription of IFN-ß is higher in THP-1 cells infected with the Δ*cdnP** mutant as compared to those infected with the WT and WTbk controls (Figure 4A). This increase in IFN-ß induction is not due to difference in bacterial growth rate, phagocytosis or intracellular killing, and is specific since TNF-α induction is similar between Δ*cdnP** and WT bacteria (Figures S4A-D).

To characterize the respective role of GBS DNA and c-di-AMP on type I IFN induction, cGAS$^{-/-}$ and STING$^{-/-}$ THP-1 cells were infected with the same strains. As observed previously (Figure 1), IFN-ß induction and IP-10 production by the GBS WT and WTbk controls is similarly decreased in both cGAS$^{-/-}$ and STING$^{-/-}$ cell lines, with a 64-70% and 70-75% decrease respectively (Figure 4B-E), confirming that cGAS is the main DNA sensor involved in IFN-ß induction in response to WT bacteria.

In the same conditions, the Δ*cdnP** mutant induced 1.6 to 2 times more IFN-ß in WT and cGAS$^{-/-}$ THP-1 cells compared with WT GBS strains (Figure 4B). The decreased IFN induction between WT and cGAS$^{-/-}$ THP-1 cells in response to the Δ*cdnP** mutant (around 64%) is similar to the one observed with the WT bacteria controls (Figure 4B). Similar results were obtained by quantifying the production of the related IP-10 cytokine by ELISA (Figure 4C). These results indicate that the relative contribution of DNA sensing by cGAS is not affected by CdnP inactivation.

In contrast, we observed a similar low level of IFN-ß induction and IP-10 production by WT bacteria and the Δ*cdnP** mutant when using STING$^{-/-}$ THP-1 cells (Figures 4C and 4D). The absence of a difference between WT and mutated bacteria in STING$^{-/-}$ THP-1 cells demonstrates that the increased IFN-ß induction is cGAS-independent and STING-dependent, suggesting a role for c-di-AMP in increased IFN-ß induction by Δ*cdnP**. Indeed, cell transfection with c-di-AMP results in IFN-ß induction and IP-10 production in WT and cGAS$^{-/-}$ THP-1 cells (Figures 4B and 4C) but not in STING$^{-/-}$ cells (Figures 4D and 4E). Similarly, incubation of digitonin-permeabilized THP-1 cells with a nucleotide fraction of GBS supernatants results in IFN-ß induction only with Δ*cdnP** supernatants (Figure S2C). Addition of rCdnP to the purified Δ*cdnP** supernatant or inactivation of STING abolished IFN-ß induction (Figure S2C). These results demonstrate that THP-1 cells induce more IFN-ß in response to infection with the Δ*cdnP**

mutant, and that this increase response is dependent on STING and on the increased amount of c-di-AMP present outside the mutated bacteria.

The same experiments were repeated in BMDMs to confirm the conserved role of c-di-AMP in IFN-ß induction. As observed with THP-1 cells, the Δ*cdnP** mutant induced IFN-ß by a cGAS and STING-dependent pathway similar to the WT GBS but, in addition, activated a cGAS-independent and STING-dependent pathway that accounts for the increased IFN-ß induction of the mutated strain (Figure 4F and 4G). In both cell lines, no difference in phagocytosis, intracellular killing, and TNF-α induction was observed for the three GBS strains in WT and mutated cell lines (Figure S4). Overall, we conclude that the Δ*cdnP** mutant induces a stronger IFN-ß response due to the cumulative effect of DNA recognition by cGAS, and c-di-AMP by a STING-dependent pathway. The DNA-cGAS pathway is similarly activated by the WT and the Δ*cdnP** mutant, while the c-di-AMP-STING pathway is activated only by the Δ*cdnP** mutant.

CdnP inactivation induces higher IFN-ß levels *in vivo* and reduces GBS virulence

Type I IFN is important for controlling GBS infection in mice (Mancuso et al., 2007) and our results showed that the GBS Δ*cdnP** mutant induced higher IFN-ß levels in THP-1 and BMDMs. To test the effect of CdnP inactivation *in vivo*, we infected WT, cGAS$^{-/-}$ and STING$^{-/-}$ mice with GBS WT, WTbk, and the Δ*cdnP** mutant. Consistent with our *in vitro* results, the Δ*cdnP** mutant induced higher IFN-ß production in WT and cGAS$^{-/-}$ mice, but not in STING$^{-/-}$ mice, when compared to WT and WTbk bacteria (Figure 5A). The difference in IFN-ß induction observed with the Δ*cdnP** mutant appears specific since TNF-α induction is not affected by CdnP inactivation in the three mice backgrounds (Figure 5B). Interestingly, inactivation of cGAS or STING decreased the absolute level of IFN-ß induction for the three GBS strains, demonstrating the important role of the cGAS-STING pathway during *in vivo* infection (Figure

12

5A).

To confirm the link between IFN-ß level and the control of GBS infection, we quantified the number of bacteria in the blood and spleen. The WT and cGAS^{-/-} mice, but not the STING^{-/-} mice, infected by the Δ*cdnP** mutant showed decreased bacteremia in both blood (Figure 5C) and spleen (Figure 5D) at 24 hours post-infection. Moreover cGAS or STING inactivation increased bacteremia, demonstrating their role to restrict bacterial infection by GBS (Figure 5C and D). In conclusion, CdnP inactivation results in higher IFN-ß induction in mice and allows a more efficient control of the infection by a STING-dependent pathway. It is therefore likely that GBS expresses CdnP at its surface to degrade its own released c-di-AMP and to promote its virulence.

DISCUSSION

Type I IFNs are better known for their role in antiviral host defense, but they are likewise important in the host response to bacterial infection with favorable or detrimental outcomes to the host depending on the pathogen (McNab et al., 2015; Monroe et al., 2010). Both viral and bacterial intracellular pathogens have been reported to induce type I IFNs by the cGAS/STING axis (Barber, 2014; Cai et al., 2014). Given the conserved and ancient origin of this signaling pathway (Kranzusch et al., 2015), it is likely that microbes have developed mechanisms to manipulate this innate immune sensing pathway. Consistently, viruses express specific proteins that increase infectiveness by interfering with cGAS or STING activation (Paludan, 2015; Wu et al., 2015; Ma and Damania, 2016).

In this study, we demonstrated that type I IFN induction by the extracellular pathogen GBS is also dependent on the cGAS/STING axis. We identified cGAS as the main upstream sensor leading to IFN-ß production in response to WT GBS, in agreement with our previous study showing that GBS DNA is the main agonist of this response (Charrel-Dennis et al., 2008).

However, we identified that WT GBS expresses a CdnP ectonucleotidase that degrades c-di-AMP outside the bacteria. Inactivation of CdnP leads to c-di-AMP accumulation outside GBS, higher levels of IFN-β *in vitro* and *in vivo*, and reduced virulence, with lower bacterial burden in infected organs. The overproduction of IFN-ß is STING-dependent but cGAS-independent, showing that bacterial cdN can activate STING either directly or with the help of additional cdN receptors such as DDX41 (Danilchanka and Mekalanos, 2013; Parvatiyar et al., 2012). By degrading its own c-di-AMP, GBS avoids the overactivation of STING, limits IFN-ß induction, and promotes its virulence.

To the best of our knowledge, a cdN catabolic activity at the bacterial surface has never been reported, or tested, in any species. Interestingly, CdnP is an enzyme belonging to the widespread ectonucleotidase family usually involved in nucleotide catabolism at the cell surface of prokaryotic and eukaryotic cells (Matange et al., 2015; Zimmermann et al., 2012). This family of enzymes is structurally unrelated to the currently known bacterial cdN phosphodiesterases, which are all involved in the regulation of the intracellular concentration of cdN to control bacterial physiology (Corrigan and Grundling, 2013; Romling et al., 2013). The current functional annotation in databases of CdnP suggests an activity on 2',3' cyclic nucleotides. Although enzymes with this predicted activity are widespread, their biological functions are unknown (Matange et al., 2015; Wilson et al., 2012) probably because the predicted 2',3' cNMP substrates have never been detected *in vivo* and are unstable intermediates that do not require a specific enzyme for their degradation (Rao et al., 2010). The CdnP activity on 3',5' cdN is therefore more likely to be a relevant physiological function instead of the activity on 2',3' cNMPs. CdnP is active on specific cdNs, being more potent on c-di-AMP, the only cdN synthesized by GBS, and unable to cleave the eukaryotic 2'3' cGAMP. Following this original CdnP enzymatic characterization, it is expected that other annotated 2',3' cNMP-degrading

enzymes are in fact phosphodiesterases acting on specific cdNs.

Prior to this study, CdnP homologues in bacteria were identified but their biological functions have been elusive. The best-characterized homologue to date is the *Vibrio cholera* CdpB enzyme necessary for bacterial growth when extracellular DNA is the only phosphate source (McDonough et al., 2015), but the nutritional function of extracellular cdN is unlikely. The secretion or release of cdNs by bacteria is common and might be a way to regulate the intracellular pool of cdN in response to environmental stresses. However, cdNs have no known function outside bacteria. No effect on GBS growth was observed by inactivating CdnP, suggesting that the extracellular accumulation of c-di-AMP has no apparent physiological role in the tested conditions. In contrast, intracellular c-di-AMP synthesis is essential for bacterial growth in almost all conditions (Corrigan and Grundling, 2013; Whiteley et al., 2015) and we were unable to inactivate the only c-di-AMP synthase gene in GBS with our conventional methods (data not shown), suggesting that c-di-AMP synthesis is indeed essential for growth in standard condition.

The biological significance of having a dedicated c-di-AMP phosphodiesterase at the GBS surface becomes relevant when considering the host-pathogen relationship (Danilchanka and Mekalanos, 2013). We found that IFN-ß induction by GBS-infected human and murine cells is dependent on cGAS, in agreement with GBS DNA as the main inducer of this TLR-independent response (Charrel-Dennis et al., 2008). This result is also consistent with cGAS activation by DNA as predominant over bacterial cdN activation of STING, as observed recently with *M. tuberculosis* (Collins et al., 2015; Wassermann et al., 2015; Watson et al., 2015), *L. monocytogenes* (Hansen et al., 2014), and *C. trachomatis* (Zhang et al., 2014). However, by inactivating CdnP in GBS, IFN-ß induction is increased and results from the additive effect on STING of the cGAS-synthesized 2'3' cGAMP in response to DNA and of the secreted bacterial c-

di-AMP (Figure 6). The increased amount of cdN outside bacteria has been previously linked to an increase in STING-dependent IFN-ß induction (Barker et al., 2013; Dey et al., 2015; Schwartz et al., 2012; Woodward et al., 2010). Interestingly, we did not detect a CdnP homologue in *L. monocytogenes*. This is not surprising since IFN-ß production has mainly negative effects on the host during infections by intracellular bacterial pathogens. It might even be possible that this pathogen class positively regulates the secretion of cdN to increase IFN-ß production. In contrast, IFN-ß is necessary for host protection against GBS and related pathogens. It is therefore advantageous for GBS to diminish STING activation by degrading c-di-AMP to promote invasion and organ colonization.

In conclusion, we extend the role of the cGAS-STING axis to the extracellular bacterial pathogen *S. agalactiae* and identified cGAS as the main sensor leading to IFN-ß production by infected macrophages. We also uncovered that wild-type GBS dampens IFN-ß production by degrading c-di-AMP due to the CdnP activity, thus avoiding the direct activation of STING. Our discovery shows the importance of c-di-AMP in the host immune response to GBS infection, and suggests that the development of CdnP inhibitors could be envisioned as a treatment strategy for infectious diseases.

EXPERIMENTAL PROCEDURES

Ethics Statement

All experiments involving animals were performed in accordance with guidelines set forth by the American Association for Laboratory Animal Science (AALAS) and were approved by the Institutional Animal Care and Use Committee (IACUC A-1332) at the University of Massachusetts Medical School (UMMS).

Bacterial strains and growth conditions

GBS strains used in this study are derivatives of NEM316, a ST-23 and serotype III clinical isolate (Glaser et al., 2002). The Δ*cylE* non-hemolytic and the Δ*nudP* deletion mutant were described previously (Firon et al., 2014; Firon et al., 2013). The Δ*cdnP** mutant was constructed, as described in the supplemental experimental procedures, by mutating the His_{199}-encoding codon to an Ala-encoding codon. The marker-less substitution and the isogenic WTbk control were confirmed by sequencing. Liquid cultures were maintained at 37°C in TH broth (TH, Difco-BD) or in a chemically defined medium (CDM).

Cells, cultures, and infections

WT, $cGAS^{-/-}$, $STING^{-/-}$ and $IFI16^{-/-}$ THP-1 cells generated with CRISPR-Cas9 (Supplemental procedures and Figure S1) were grown in RPMI1640 supplemented with 4 mM glutamine and 10% FBS. Primary BMDMs from C57BL/6 mice were generated as described previously (Charrel-Dennis et al., 2008) and cultured in Dulbecco's modified Eagle's medium (DMEM; Gibco-BRL) supplemented with 4 mM glutamine and 10% FBS. $cGAS^{-/-}$ and $STING^{-/-}$ mice were obtained from G. Barber (University of Miami). Cells were infected with live GBS cultures as described (Charrel-Dennis et al., 2008) at an MOI of 6, unless otherwise stated. Cells were harvested 6 to 18 hrs post-infection for RNA preparation and supernatant analysis.

Quantitative RT-PCR and ELISA

Total RNA was extracted from infected cells using Trizol (Invitrogen) and one microgram of total RNAs was used for cDNA synthesis and quantitative PCR (Bio-Rad). Levels of human and mouse IFN-ß and TNF-α were normalized against their respective GAPDH housekeeping genes. Quantification by ELISA was performed on cell supernatants after the indicated time of infection as described for mouse IFN-ß (Roberts et al., 2007) and according to the manufacturer's

instructions (R&D Research) for human CXCL10/IP-10 and mouse and human TNF-α.

Quantification of GBS intracellular cdN by LC-MS/MS

Quantification of cdNs was performed by LC-MS/MS by BioLog Life Science GmbH using internal labeled standards. Extraction of cdNs on 5 ml of overnight GBS cultures was performed with Acetonitrile / Methanol / Water (2/2/1, v/v/v) buffer as recommended. Quantities of cdNs were normalized against the quantity of total protein extract.

Quantification of cdN and nucleotides by RR-HPLC

Rapid Resolution High Performance Liquid Chromatography (RR-HPLC) was used to determine kinetics of extracellular c-di-AMP degradation on whole GBS cells, extracellular c-di-AMP quantification, and for CdnP enzymatic characterization as described in supplemental experimental procedures. Reagents and standards were purchased from BioLog Life Sciences GmbH (c-di-AMP, c-di-GMP, cGAMP, 2'3' cGAMP, 2',3' and 3',5' cyclic NMPs) or from Sigma Aldrich (NMP, NDP, nucleotides, nucleosides).

Extracellular c-di-AMP degradation by GBS

GBS in early stationary phase were incubated with 0.1 mM c-di-AMP in 50 mM Tris and 5 mM $MnCl_2$, at 37°C with agitation. Aliquots were taken at different times, centrifuged two times to eliminate bacteria, and the kinetics of c-di-AMP degradation and product formation was analyzed by RR-HPLC.

Quantification of extracellular c-di-AMP in GBS supernatants

Enrichment of c-di-AMP was done by affinity purification on 40 ml of GBS supernatants with the c-di-AMP binding protein CabP (Bai et al., 2014), as detailed in the supplemental experimental procedure. Relative quantification of extracellular c-di-AMP was performed by RR-HPLC with an external standard (40 ml of PBS containing 1.25 μM c-di-AMP) treated in the same condition to normalize samples.

Characterization of rCdnP enzymatic activities

Recombinant CdnP (residues 29-768) was produced in *E. coli* and analyzed by ultracentrifugation (An60Ti rotor, Beckman Coulter) as described in the supplemental experimental procedures. The rCdnP metallo-phosphatase activities were first assayed on 2',3' cyclic nucleotides by measuring the release of inorganic phosphate (P_i) with Malachite Green reagent (*BIOMOL GREEN*[TM], Enzo Life Sciences). Inorganic phosphate (P_i) was quantified (absorbance at 620 nm) against a standard P_i curve. Kinetics with cdNs were done at 37°C in 50 mM Tris, pH 7.5, containing 5 mM $MnCl_2$, 100-200 μM of substrates and 3 nM purified rCdnP enzyme. Substrate degradation and product formation were followed every 7 min by RR-HPLC.

***In vivo* infection and bacterial burden**

6-week-old female C57BL/6 mice (Charles River) were injected intravenously with 1.5×10^7 CFUs of bacteria harvested during the exponential growth phase, washed in PBS, and resuspended in 100 μl. At 12 and 24 hrs after infection, mice were bled to evaluate serum IFN-ß levels. Bacterial counts in blood and spleen homogenates were determined by plating serial dilutions on blood agar plates.

Statistical Analysis

All *in vitro* data were analyzed using an unpaired, two-tailed Student's t test with a 95% confidence interval. *In vivo* data were analyzed using a non-parametric ANOVA (Kruskal-Wallis) (Prism; GraphPad Software, Inc.). Data are represented as means ± SD.

Author contributions

W.A.A., A.F., P.T.C, D.T.G. and P.A.K. conceived and designed experiments. W.A.A., A.F., T.S., and P.A.K performed experiments. V.H., and K.A.F provided reagents. W.A.A., A.F., E.K.J., P.T.C, D.T.G. and P.A.K. analyzed data. W.A.A., A.F., P.T.C, D.T.G. and P.A.K. wrote the paper.

Acknowledgments

References

Ablasser, A., Goldeck, M., Cavlar, T., Deimling, T., Witte, G., Rohl, I., Hopfner, K.P., Ludwig, J., and Hornung, V. (2013). cGAS produces a 2'-5'-linked cyclic dinucleotide second messenger that activates STING. Nature *498*, 380-384.

Anraku, Y. (1964). A New Cyclic Phosphodiesterase Having a 3'-Nucleotidase Activity from *Escherichia Coli* B. II. Further Studies on Substrate Specificity and Mode of Action of the Enzyme. J Biol Chem *239*, 3420-3424.

Archer, K.A., Durack, J., and Portnoy, D.A. (2014). STING-dependent type I IFN production inhibits cell-mediated immunity to *Listeria monocytogenes*. PLoS pathogens *10*, e1003861.

Bai, Y., Yang, J., Zarrella, T.M., Zhang, Y., Metzger, D.W., and Bai, G. (2014). Cyclic di-AMP impairs potassium uptake mediated by a cyclic di-AMP binding protein in *Streptococcus pneumoniae*. Journal of bacteriology *196*, 614-623.

Barber, G.N. (2014). STING-dependent cytosolic DNA sensing pathways. Trends in immunology *35*, 88-93.

Barker, J.R., Koestler, B.J., Carpenter, V.K., Burdette, D.L., Waters, C.M., Vance, R.E., and Valdivia, R.H. (2013). STING-dependent recognition of cyclic di-AMP mediates type I interferon responses during *Chlamydia trachomatis* infection. mBio *4*, e00018-00013.

Burdette, D.L., Monroe, K.M., Sotelo-Troha, K., Iwig, J.S., Eckert, B., Hyodo, M., Hayakawa, Y., and Vance, R.E. (2011). STING is a direct innate immune sensor of cyclic di-GMP. Nature *478*, 515-518.

Cai, X., Chiu, Y.H., and Chen, Z.J. (2014). The cGAS-cGAMP-STING pathway of cytosolic DNA sensing and signaling. Mol Cell *54*, 289-296.

Charrel-Dennis, M., Latz, E., Halmen, K.A., Trieu-Cuot, P., Fitzgerald, K.A., Kasper, D.L., and Golenbock, D.T. (2008). TLR-independent type I interferon induction in response to an

extracellular bacterial pathogen via intracellular recognition of its DNA. Cell Host Microbe *4*, 543-554.

Collins, A.C., Cai, H., Li, T., Franco, L.H., Li, X.D., Nair, V.R., Scharn, C.R., Stamm, C.E., Levine, B., Chen, Z.J.*, et al.* (2015). Cyclic GMP-AMP Synthase Is an Innate Immune DNA Sensor for *Mycobacterium tuberculosis*. Cell Host Microbe *17*, 820-828.

Corrigan, R.M., and Grundling, A. (2013). Cyclic di-AMP: another second messenger enters the fray. Nat Rev Microbiol *11*, 513-524.

Danilchanka, O., and Mekalanos, J.J. (2013). Cyclic dinucleotides and the innate immune response. Cell *154*, 962-970.

Davies, B.W., Bogard, R.W., Young, T.S., and Mekalanos, J.J. (2012). Coordinated Regulation of Accessory Genetic Elements Produces Cyclic Di-Nucleotides for *V. cholerae* Virulence. Cell *149*, 358-370.

Dey, B., Dey, R.J., Cheung, L.S., Pokkali, S., Guo, H., Lee, J.H., and Bishai, W.R. (2015). A bacterial cyclic dinucleotide activates the cytosolic surveillance pathway and mediates innate resistance to tuberculosis. Nat Med *21*, 401-406.

Firon, A., Dinis, M., Raynal, B., Poyart, C., Trieu-Cuot, P., and Kaminski, P.A. (2014). Extracellular nucleotide catabolism by the Group B *Streptococcus* ectonucleotidase NudP increases bacterial survival in blood. J Biol Chem *289*, 5479-5489.

Firon, A., Tazi, A., Da Cunha, V., Brinster, S., Sauvage, E., Dramsi, S., Golenbock, D.T., Glaser, P., Poyart, C., and Trieu-Cuot, P. (2013). The Abi-domain protein Abx1 interacts with the CovS histidine kinase to control virulence gene expression in group B *Streptococcus*. PLoS Pathog *9*, e1003179.

Gao, P., Ascano, M., Wu, Y., Barchet, W., Gaffney, B.L., Zillinger, T., Serganov, A.A., Liu, Y., Jones, R.A., Hartmann, G.*, et al.* (2013a). Cyclic [G(2',5')pA(3',5')p] is the metazoan second messenger produced by DNA-activated cyclic GMP-AMP synthase. Cell *153*, 1094-1107.

Gao, P., Ascano, M., Zillinger, T., Wang, W., Dai, P., Serganov, A.A., Gaffney, B.L., Shuman, S., Jones, R.A., Deng, L.*, et al.* (2013b). Structure-function analysis of STING activation by c[G(2',5')pA(3',5')p] and targeting by antiviral DMXAA. Cell *154*, 748-762.

Glaser, P., Rusniok, C., Buchrieser, C., Chevalier, F., Frangeul, L., Msadek, T., Zouine, M., Couve, E., Lalioui, L., Poyart, C.*, et al.* (2002). Genome sequence of *Streptococcus agalactiae*, a pathogen causing invasive neonatal disease. Mol Microbiol *45*, 1499-1513.

Gratz, N., Hartweger, H., Matt, U., Kratochvill, F., Janos, M., Sigel, S., Drobits, B., Li, X.D., Knapp, S., and Kovarik, P. (2011). Type I interferon production induced by *Streptococcus* pyogenes-derived nucleic acids is required for host protection. PLoS Pathog *7*, e1001345.

Hansen, K., Prabakaran, T., Laustsen, A., Jorgensen, S.E., Rahbaek, S.H., Jensen, S.B., Nielsen, R., Leber, J.H., Decker, T., Horan, K.A.*, et al.* (2014). *Listeria monocytogenes* induces IFN expression through an IFI16-, cGAS- and STING-dependent pathway. The EMBO Journal *33*, 1654-1666.

Joubrel, C., Tazi, A., Six, A., Dmytruk, N., Touak, G., Bidet, P., Raymond, J., Trieu-Cuot, P., Fouet, A., Kerneis, S.*, et al.* (2015). Group B *Streptococcus* neonatal invasive infections, France 2007-2012. Clin Microbiol Infect *21*, 910-916.

Kranzusch, P.J., Wilson, S.C., Lee, A.S., Berger, J.M., Doudna, J.A., and Vance, R.E. (2015). Ancient Origin of cGAS-STING Reveals Mechanism of Universal 2',3' cGAMP Signaling. Molecular Cell *59*, 891-903.

Ma, Z., and Damania, B. (2016). The cGAS-STING Defense Pathway and Its Counteraction by Viruses. Cell Host Microbe *19*, 150-158.

Mancuso, G., Midiri, A., Biondo, C., Beninati, C., Zummo, S., Galbo, R., Tomasello, F., Gambuzza, M., Macri, G., Ruggeri, A*., et al.* (2007). Type I IFN signaling is crucial for host resistance against different species of pathogenic bacteria. J Immunol *178*, 3126-3133.

Manzanillo, P.S., Shiloh, M.U., Portnoy, D.A., and Cox, J.S. (2012). *Mycobacterium Tuberculosis* Activates the DNA-Dependent Cytosolic Surveillance Pathway within Macrophages. Cell Host Microbe *11*, 469-480.

Matange, N., Podobnik, M., and Visweswariah, S.S. (2015). Metallophosphoesterases: structural fidelity with functional promiscuity. Biochem J *467*, 201-216.

McDonough, E., Kamp, H., and Camilli, A. (2015). *Vibrio cholerae* phosphatases required for the utilization of nucleotides and extracellular DNA as phosphate sources. Mol Microbiol.

McNab, F., Mayer-Barber, K., Sher, A., Wack, A., and O'Garra, A. (2015). Type I interferons in infectious disease. Nat Rev Immunol *15*, 87-103.

McWhirter, S.M., Barbalat, R., Monroe, K.M., Fontana, M.F., Hyodo, M., Joncker, N.T., Ishii, K.J., Akira, S., Colonna, M., Chen, Z.J*., et al.* (2009). A host type I interferon response is induced by cytosolic sensing of the bacterial second messenger cyclic-di-GMP. J Exp Med *206*, 1899-1911.

Monroe, K.M., McWhirter, S.M., and Vance, R.E. (2010). Induction of type I interferons by bacteria. Cell Microbiol *12*, 881-890.

Oliveira, L., Madureira, P., Andrade, E.B., Bouaboud, A., Morello, E., Ferreira, P., Poyart, C., Trieu-Cuot, P., and Dramsi, S. (2012). Group B *streptococcus* GAPDH is released upon cell lysis, associates with bacterial surface, and induces apoptosis in murine macrophages. PLoS One *7*, e29963.

Paludan, S.R. (2015). Activation and regulation of DNA-driven immune responses. Microbiol Mol Biol Rev *79*, 225-241.

Parker, D., Planet, P.J., Soong, G., Narechania, A., and Prince, A. (2014). Induction of type I interferon signaling determines the relative pathogenicity of *Staphylococcus aureus* strains. PLoS Pathog *10*, e1003951.

Parvatiyar, K., Zhang, Z., Teles, R.M., Ouyang, S., Jiang, Y., Iyer, S.S., Zaver, S.A., Schenk, M., Zeng, S., Zhong, W*., et al.* (2012). The helicase DDX41 recognizes the bacterial secondary messengers cyclic di-GMP and cyclic di-AMP to activate a type I interferon immune response. Nat Immunol *13*, 1155-1161.

Rao, F., Qi, Y., Murugan, E., Pasunooti, S., and Ji, Q. (2010). 2',3'-cAMP hydrolysis by metal-dependent phosphodiesterases containing DHH, EAL, and HD domains is non-specific: Implications for PDE screening. Biochem Biophys Res Commun *398*, 500-505.

Roberts, Z.J., Goutagny, N., Perera, P.Y., Kato, H., Kumar, H., Kawai, T., Akira, S., Savan, R., van Echo, D., Fitzgerald, K.A*., et al.* (2007). The chemotherapeutic agent DMXAA potently and specifically activates the TBK1-IRF-3 signaling axis. J Exp Med *204*, 1559-1569.

Romling, U., Galperin, M.Y., and Gomelsky, M. (2013). Cyclic di-GMP: the First 25 Years of a Universal Bacterial Second Messenger. Microbiol Mol Biol Rev *77*, 1-52.

Schwartz, K.T., Carleton, J.D., Quillin, S.J., Rollins, S.D., Portnoy, D.A., and Leber, J.H. (2012). Hyperinduction of host beta interferon by a *Listeria monocytogenes* strain naturally overexpressing the multidrug efflux pump MdrT. Infect Immun *80*, 1537-1545.

Wassermann, R., Gulen, M.F., Sala, C., Perin, S.G., Lou, Y., Rybniker, J., Schmid-Burgk, J.L., Schmidt, T., Hornung, V., Cole, S.T*., et al.* (2015). *Mycobacterium tuberculosis* Differentially Activates cGAS- and Inflammasome-Dependent Intracellular Immune Responses through ESX-1. Cell Host Microbe *17*, 799-810.

Watson, R.O., Bell, S.L., MacDuff, D.A., Kimmey, J.M., Diner, E.J., Olivas, J., Vance, R.E., Stallings, C.L., Virgin, H.W., and Cox, J.S. (2015). The Cytosolic Sensor cGAS Detects

Mycobacterium tuberculosis DNA to Induce Type I Interferons and Activate Autophagy. Cell Host Microbe *17*, 811-819.

Whiteley, A.T., Pollock, A.J., and Portnoy, D.A. (2015). The PAMP c-di-AMP Is Essential for *Listeria* Growth in Macrophages and Rich but Not Minimal Media due to a Toxic Increase in (p)ppGpp. Cell Host Microbe *17*, 788-798.

Wilson, S.J., Schoggins, J.W., Zang, T., Kutluay, S.B., Jouvenet, N., Alim, M.A., Bitzegeio, J., Rice, C.M., and Bieniasz, P.D. (2012). Inhibition of HIV-1 particle assembly by 2',3'-cyclic-nucleotide 3'-phosphodiesterase. Cell Host Microbe *12*, 585-597.

Woodward, J.J., Iavarone, A.T., and Portnoy, D.A. (2010). c-di-AMP secreted by intracellular *Listeria monocytogenes* activates a host type I interferon response. Science *328*, 1703-1705.

Wu, J.J., Li, W., Shao, Y., Avey, D., Fu, B., Gillen, J., Hand, T., Ma, S., Liu, X., Miley, W.*, et al.* (2015). Inhibition of cGAS DNA Sensing by a Herpesvirus Virion Protein. Cell Host Microbe *18*, 333-344.

Yamamoto, T., Hara, H., Tsuchiya, K., Sakai, S., Fang, R., Matsuura, M., Nomura, T., Sato, F., Mitsuyama, M., and Kawamura, I. (2012). *Listeria monocytogenes* strain-specific impairment of the TetR regulator underlies the drastic increase in cyclic di-AMP secretion and beta interferon-inducing ability. Infect Immun *80*, 2323-2332.

Zhang, X., Shi, H., Wu, J., Zhang, X., Sun, L., Chen, C., and Chen, Z.J. (2013). Cyclic GMP-AMP containing mixed phosphodiester linkages is an endogenous high-affinity ligand for STING. Mol Cell *51*, 226-235.

Zhang, Y., Yeruva, L., Marinov, A., Prantner, D., Wyrick, P.B., Lupashin, V., and Nagarajan, U.M. (2014). The DNA sensor, cyclic GMP-AMP synthase, is essential for induction of IFN-beta during *Chlamydia trachomatis* infection. J Immunol *193*, 2394-2404.

Zimmermann, H., Zebisch, M., and Strater, N. (2012). Cellular function and molecular structure of ecto-nucleotidases. Purinergic Signal *8*, 437-502.

Figure Legends

Figure 1. cGAS is the main mediator of IFN-ß production in response to WT GBS.

(A-C) Quantification of IFN-ß induction by qRT-PCR in human THP-1 cells and cGAS^{-/-} (A), IFI16^{-/-} (B), and STING [-/-] (C) inactivated cell lines following 6 hrs of infection with GBS WT or the isogenic Δ*cylE* mutant (MOI-6). Transfection with DNA (3 μg/ml) was added as a control.

(D-E) Quantification of IP-10 production in THP-1 cGAS^{-/-} (D) and STING [-/-] (E) by ELISA after 18 hrs of infection.

(F-G) Quantification of IFN-ß induction using WT, cGAS^{-/-} and STING^{-/-} BMDMs at the mRNA level after 6 hrs of infection (F) or at the protein level after 18 hrs of infection (G) with GBS WT and Δ*cylE* mutant (MOI-6). An additional LPS control (100 ng/ml), independent of the cGAS-STING axis, was added.

(H-I) Same experiments as in (F-G) to quantify levels of TNF-α mRNA (H) and protein (I).

Data are represented as mean ± SD of at least three independent experiments. Asterisks indicate statistically significant differences (*,$p < 0.05$; **, $p < 0.01$ and ***, $p < 0.001$). NS, not significant. See also Figure S1.

Figure 2. CdnP degrades extracellular c-di-AMP.

(A) GBS synthesizes only c-di-AMP. The intracellular concentration of cyclic di-nucleotides was quantified by LC-MS/MS in total WT GBS extracts.

(B) GBS degrades extracellular c-di-AMP. At t = 0, 100 μM c-di-AMP was added to early stationary phase cultures of GBS previously washed and resuspend in Tris-HCl (pH 7.5)

containing 5 mM MnCl$_2$. Kinetics of extracellular c-di-AMP degradation (mean and S.D. from at least three independent bacterial cultures) were followed by RR-HPLC for the WT (black dots), the Δ*nudP* (blue triangles), and the Δ*cdnP** (red squares) ectonucleotidase mutants.

(C) Extracellular c-di-AMP is degraded into adenosine by the sequential activity of the NudP and CdnP ectonucleotidases. Same experiments as in (B) monitoring the formation of the reaction products at the end of the experiment (t = 100 min) for the WT (black), the Δ*nudP* (blue), and the Δ*cdnP** (red) ectonucleotidase mutants.

(D) Schematic representations of NudP and CdnP. The archetypal metallophosphatase (Metallophos, pfam domain 00149) and substrate-binding (5-Nucleotid_C, pfam domain 02872) domains of ectonucleotidases are colored (blue for NudP, red for CdnP). Numbers indicate the amino acid positions of the domains in the proteins. Transmembrane domains are indicated as grey boxes and are necessary for secretion (SP: signal peptide) and cell wall anchoring through the LPxTG motif (black rhombus). The black asterisk indicates the position of the conserved histidine residue at position 199 of CdnP essential for metallophosphodiesterase activity. The corresponding mutation to alanine in the catalytically inactive (*cat*⁻) mutant CdnP* is shown.

(E) CdnP activity limits extracellular c-di-AMP accumulation by GBS. Extracellular c-di-AMP in the GBS culture supernatants was quantified by an enzyme-linked assay followed by RR-HPLC. The two control GBS strains (black: WT and white: WTbk) are compared in parallel with the Δ*cdnP** mutant (red). Mean and S.D. in arbitrary units (AU) are calculated from at least three independent experiments. See also Figure S2.

Figure 3. The ectonucleotidase CdnP is a manganese-dependent c-di-AMP phosphodiesterase.

(A) Analytical ultracentrifugation analysis of rCdnP. The purified recombinant CdnP protein (residues 29–768) is a monomer with an elongated shape. Sedimentation coefficients are expressed in Svedberg units where $1 \text{ S} = 10^{-13} \text{ S}$.

(B and C) Influence of the pH and cations on the activity of CdnP. Quantification of inorganic phosphate release (P_i) was done with Biomol Green reagents after incubation of 3 nM rCdnP with 2 mM of 2',3' cUMP in the presence of 2 mM Mn^{2+} (B) or different cations at pH 7.5 (C). Samples were taken every 10 min and activities are expressed as µmol of P_i per min per mg of proteins.

(D) CdnP degrades c-di-AMP into AMP. rCdnP was incubated with c-di-AMP at 37°C. Kinetics of substrate degradation and product formation was followed by RR-HPLC. Representative chromatograms in arbitrary units (mAU) are shown.

(E) Same experiment as in (D) with the quantification of AMP formation by the rCdnP protein and the inactive rCdnP* mutant with the $H_{199}A$ substitution. See also Figure S3.

Figure 4. Increased type I interferon response by GBS Δ*cdnP** mutant is dependent on STING.

(A) THP-1 cells were infected with GBS WT, WTbk or Δ*cdnP** mutant for 4 hrs at different MOIs and IFN-ß mRNA levels were quantified by qRT-PCR and normalized to GAPDH levels. Uninfected cells (media) served as controls.

(B) Quantification of IFN-ß mRNA in WT and cGAS^{-/-} THP-1 cells after 4 hrs of infection (MOI-6) with GBS WT, WTbk, or Δ*cdnP** mutant or after transfection with c-di-AMP (100 nM).

(C) Quantification of IP-10 by ELISA in WT and cGAS^{-/-} THP-1 cells supernatants after 18 hrs of infection.

(D) Same experiment as in (B) with STING$^{-/-}$ THP-1 cells.

(E) Same experiment as in (C) with STING$^{-/-}$ THP-1 cells.

(F) Same experiment as in (B) with WT, cGAS$^{-/-}$ and STING$^{-/-}$ BMDMs.

(G) Same experiment as in (F) with the quantification of mouse IFN-ß production by ELISA after 18 hrs of infection.

All data are represented as mean ± SD of three experiments and asterisks indicate statistically significant differences (*, p < 0.05; **, p < 0.01 and ***, p < 0.001). ND, not detected. See also Figure S2 and S4.

Figure 5. GBS Δ*cdnP** mutant induces higher type I interferon response *in vivo* in both WT and cGAS$^{-/-}$, but not in STING$^{-/-}$ mice.

(A-C) WT, cGAS$^{-/-}$, and STING$^{-/-}$ mice (n = 10 for each genotype) were infected by intravenous injection with 1.5 x 10^7 CFUs of GBS WT, WTbk, or Δ*cdnP** mutant. Mice were bled 12 and 24 post-infection. Serum IFN-ß (A) and TNF-α (B) levels were measured by ELISA, and blood bacteremia was evaluated by plating serial dilutions (C).

(D) Same experimental condition as in (A-C) evaluating spleen bacteremia after 24 of infection (n = 8 for each time point).

Data are presented as mean ± SD of one of the two independent experiments that yielded similar results. Asterisks indicate that differences are statistically significant (*,p < 0.05; **, p < 0.01 and ***, p < 0.001).

Figure 6. Model of cGAS/STING activation by WT GBS and Δ*cdnP** mutant.

Top panel: WT GBS induces type I IFN by a cGAS-dependent pathway following bacterial DNA sensing, synthesis of 2'3' cGAMP, and activation of the STING / TBK1 / IRF3 axis. The c-di-AMP released by GBS is degraded by the CdnP cell wall-anchored ectonucleotidase into AMP, which is further degraded by the second ectonucleotidase NudP into adenosine (Ado).

Bottom panel: in the absence of the CdnP ectonucleotidase (GBS Δ*cdnP** mutant), c-di-AMP accumulation outside the bacteria activates STING independently of cGAS, and, together with GBS DNA sensing by cGAS, leads to type I IFN over-production.
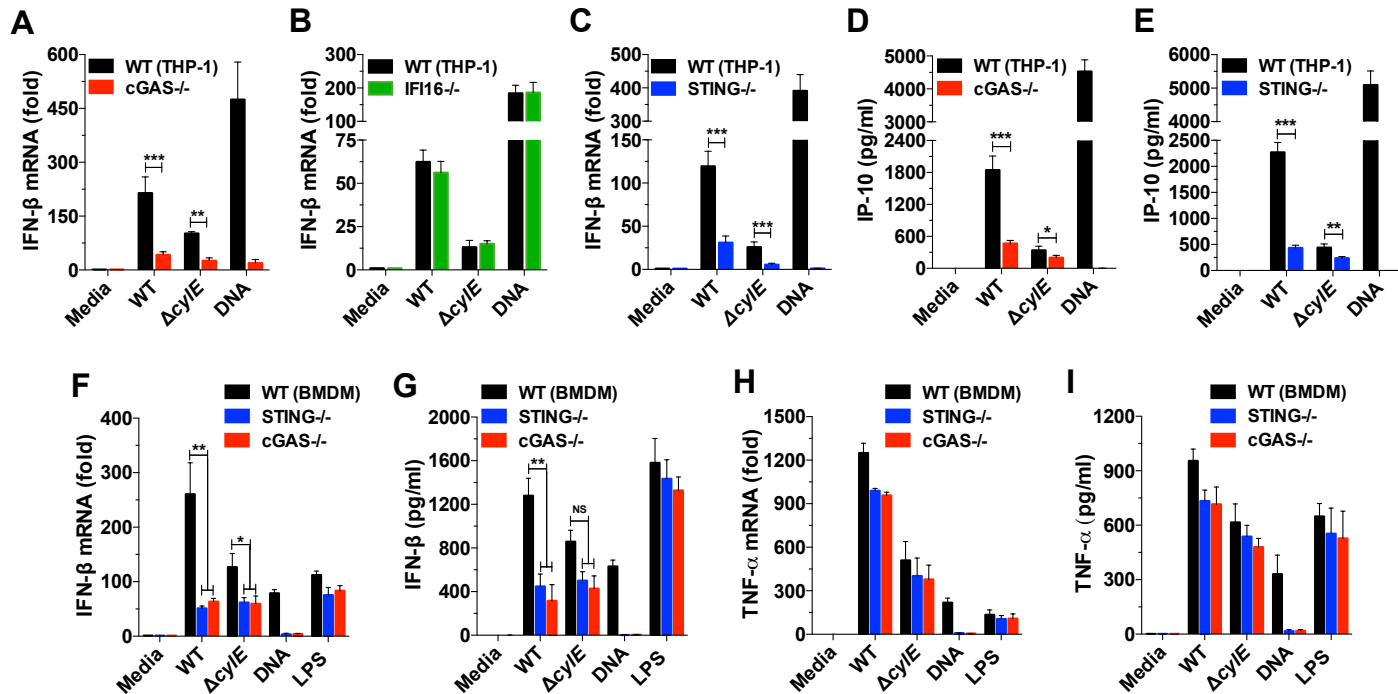
Table 1. Kinetic parameters of CdnP on cyclic mono and dinucleotides.

Substrate	Km (µM)	$Kcat$ (s^{-1})	$Kcat/Km$ (s^{-1}/M^{-1})
Cyclic nucleotide			
2',3' cGMP	22 ± 4	9.4	4.2×10^5
2',3' cUMP	42 ± 10	19.8	4.7×10^5
3',5' cAMP	n.d.	n.d.	n.d.
3',5' cGMP	n.d.	n.d.	n.d.
Cyclic dinucleotide			
c-di-AMP	14 ± 1	17.4	1.2×10^6
c-di-GMP	13.2 ± 6	2.6	1.9×10^5
c-GAMP	4.0 ± 1.6	4.5	1.1×10^6
2'3' cGAMP	n.d.	n.d.	n.d.

The V_{max} and K_m (mean ± S.D.) were obtained from double reciprocal plots of initial velocity measurements with at least five different concentrations of substrates. The k_{cat} was calculated assuming a molecular mass of 81 kDa. (n.d. = substrate hydrolysis not detected.)
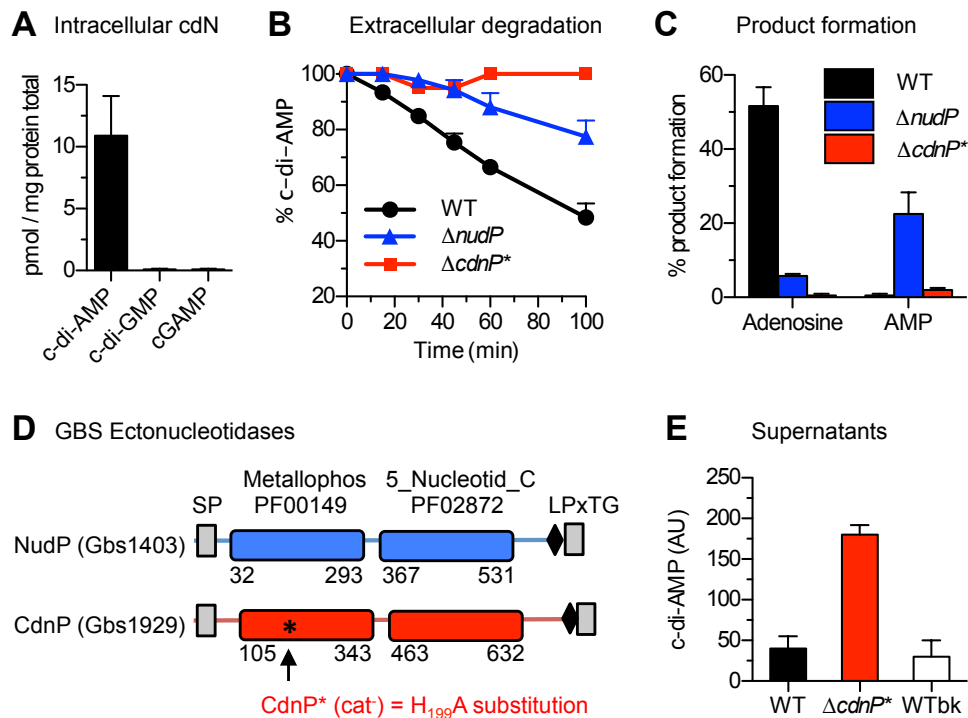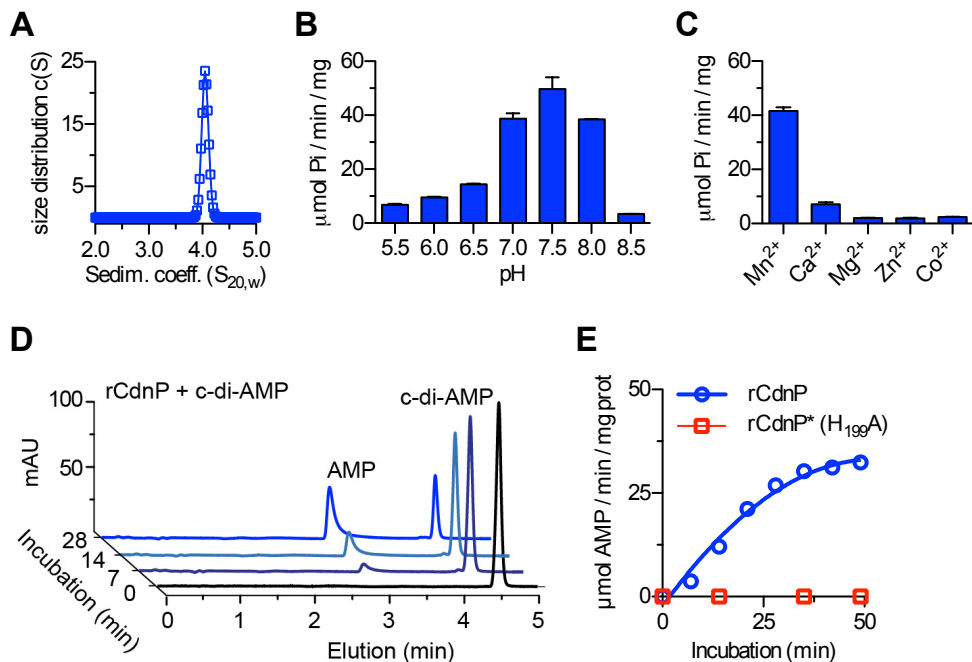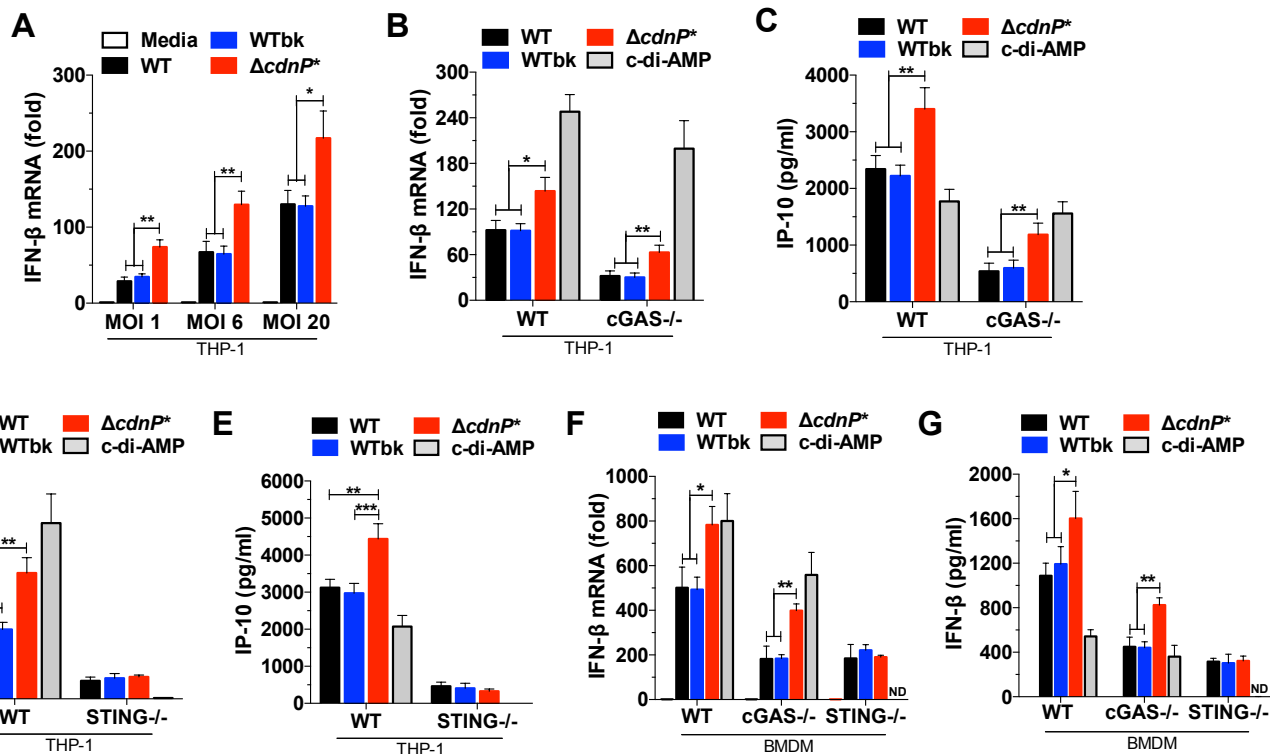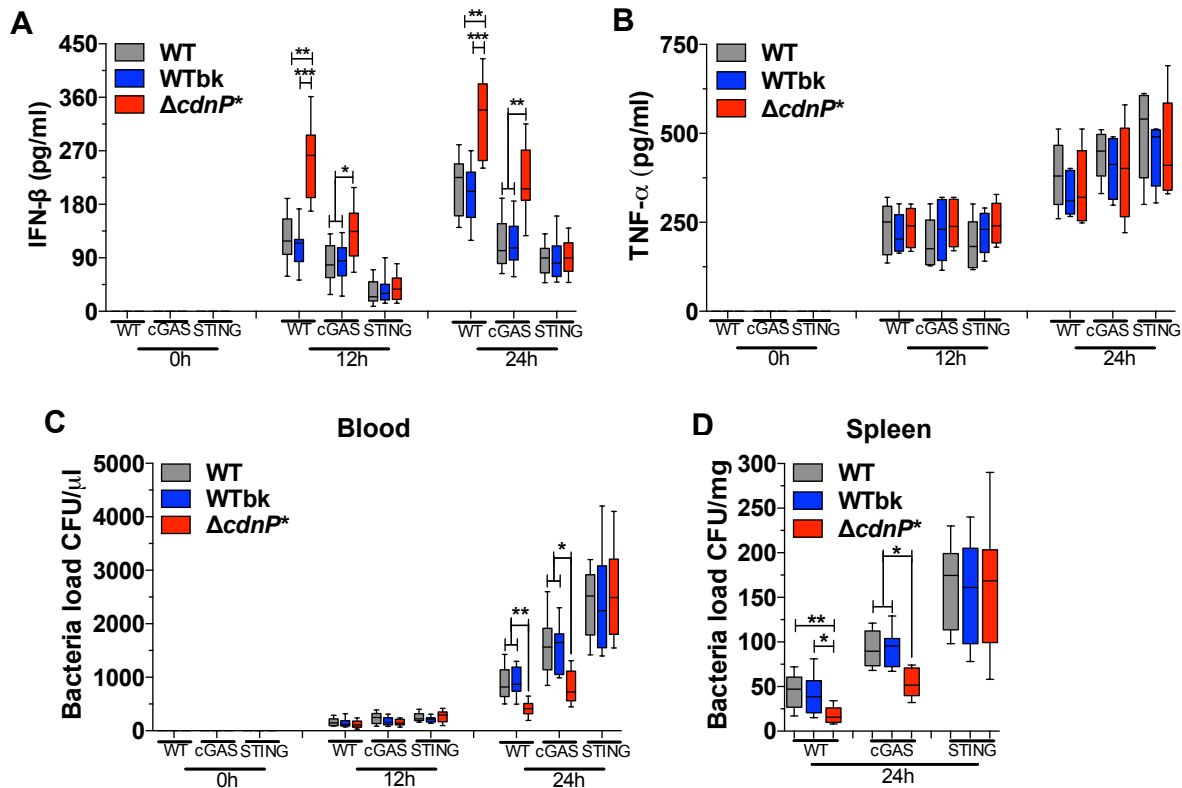
Figure 1

Figure 2

A Intracellular cdN

B Extracellular degradation

C Product formation

D GBS Ectonucleotidases

CdnP* (cat⁻) = $H_{199}A$ substitution

E Supernatants

Figure 3

A

B

C

D

rCdnP + c-di-AMP

c-di-AMP

AMP

E

Figure 4

Figure 6

Figure S1

THP1 THP1
WT STING
KO

◄STING

β-actin

A GBS supernatants

B c-di-AMP purification from GBS supenatants

C
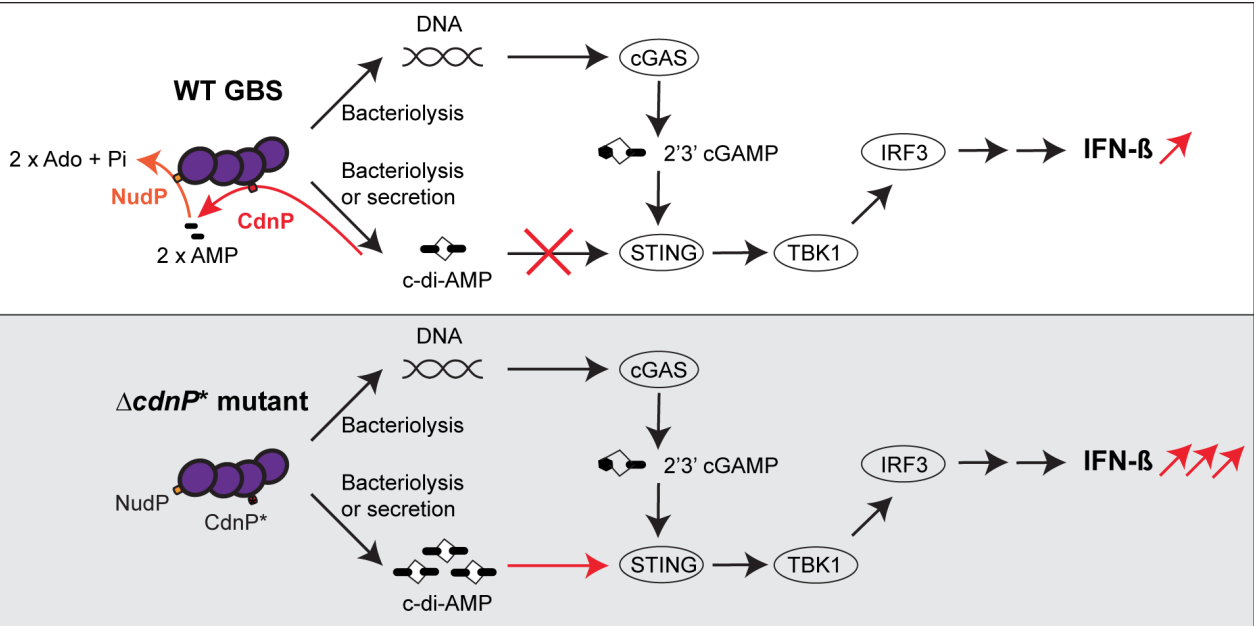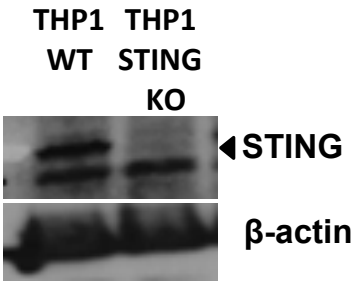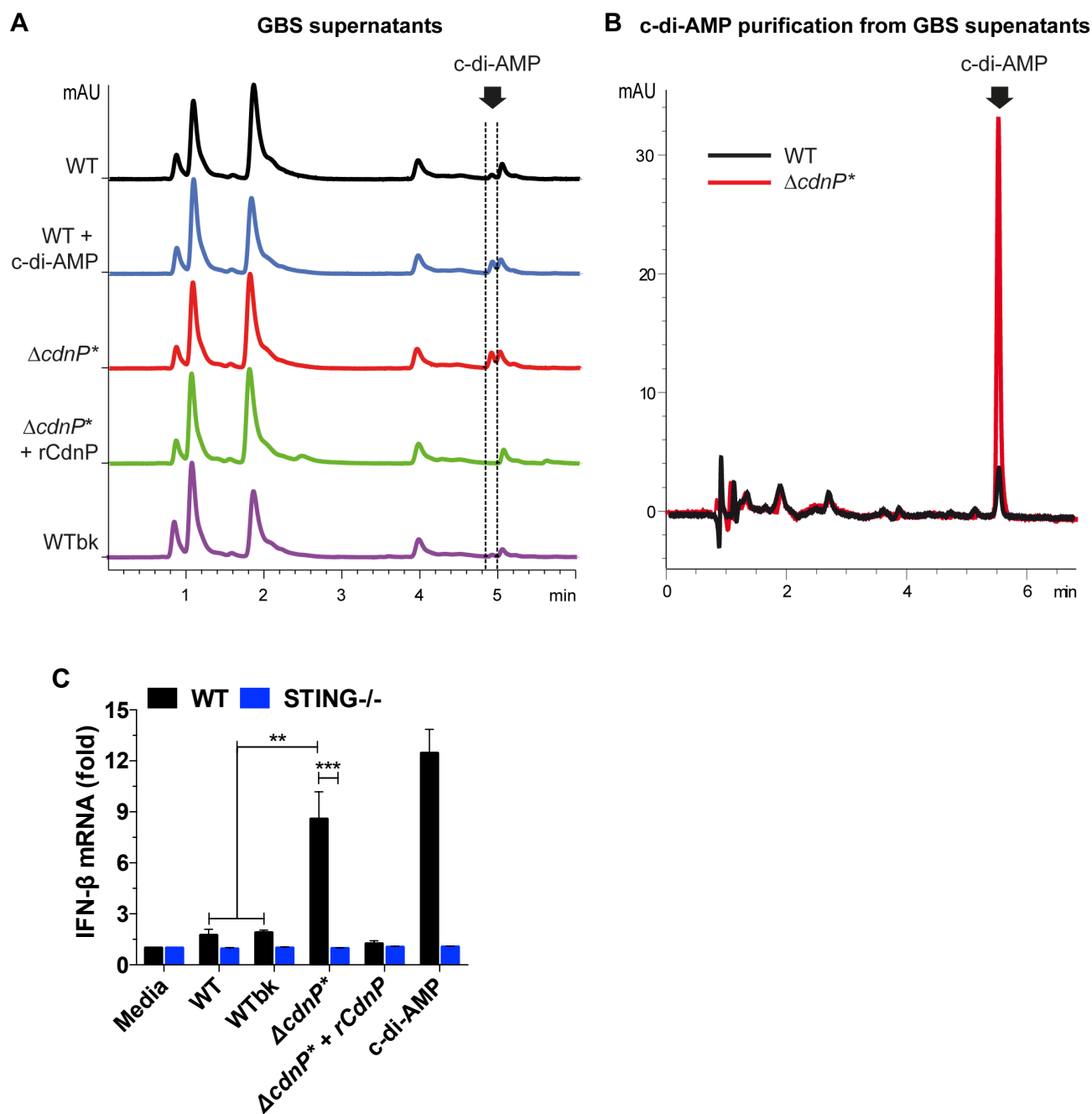
A. CdnP phosphodiesterase and nuclease activities on cyclic nucleotides

2'3' cUMP → CdnP → 2' UMP or 3' UMP → CdnP → Uridine (Pi)
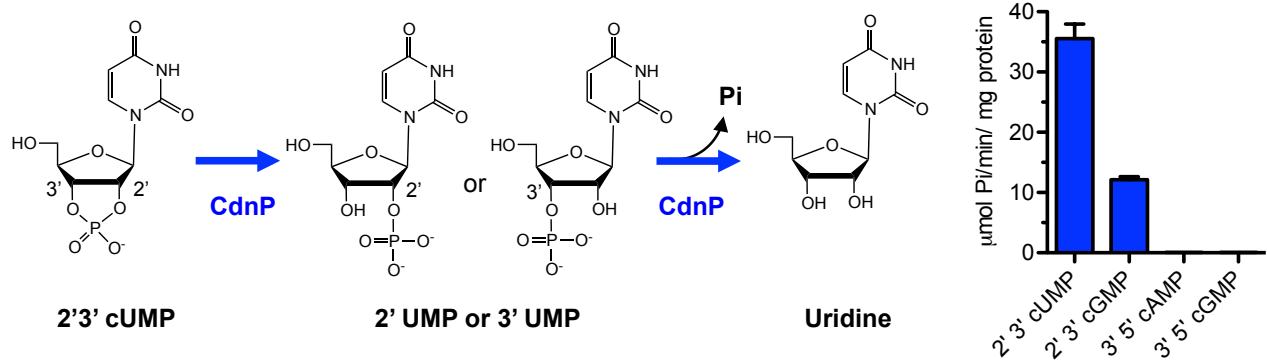
B. CdnP 3'phosphodiesterase activity on cyclic dinucleotides

c-di-AMP → CdnP → 2 x AMP → NudP → 2 x Adenosine (Pi)
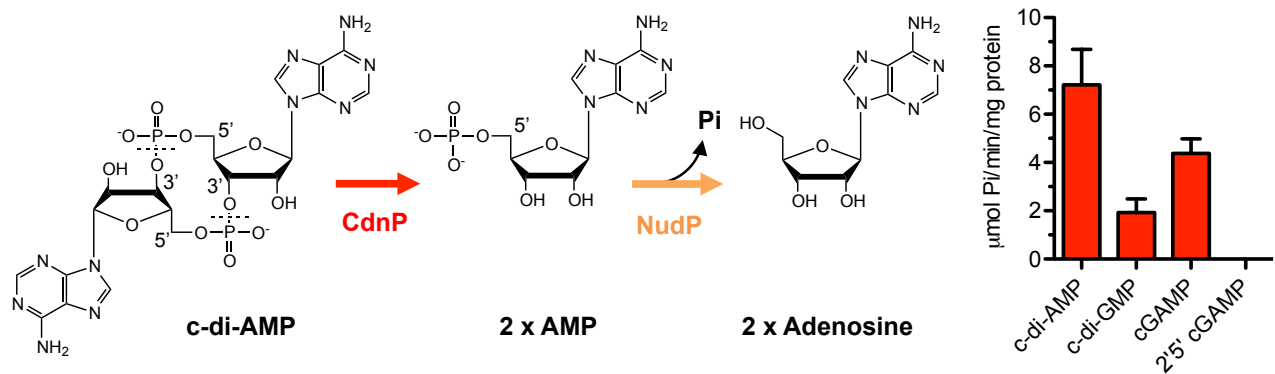
C. Inhibition of CdnP activity by non-hydrolyzable cyclic di-nucleotide analog

Rp,Rp-c-diAMPSS cc (mM)
- 0
- 0.04
- 0.05
- 0.06
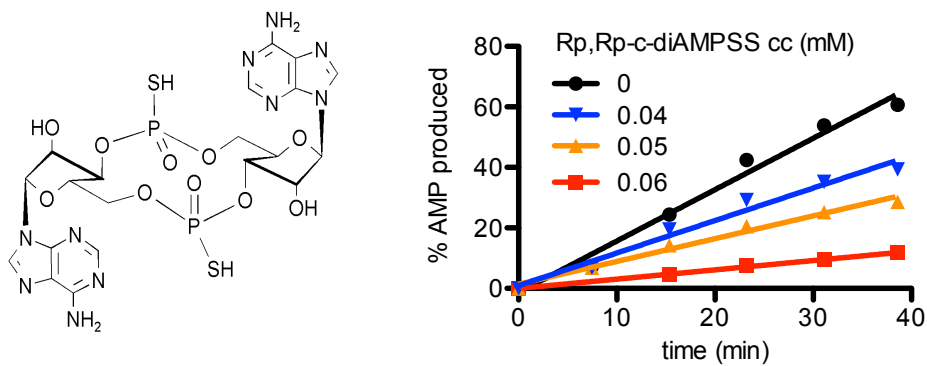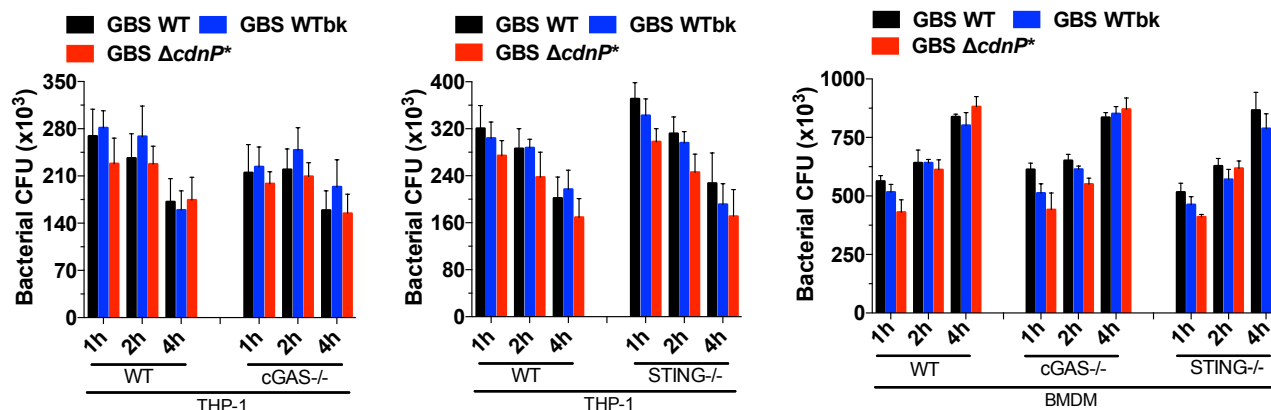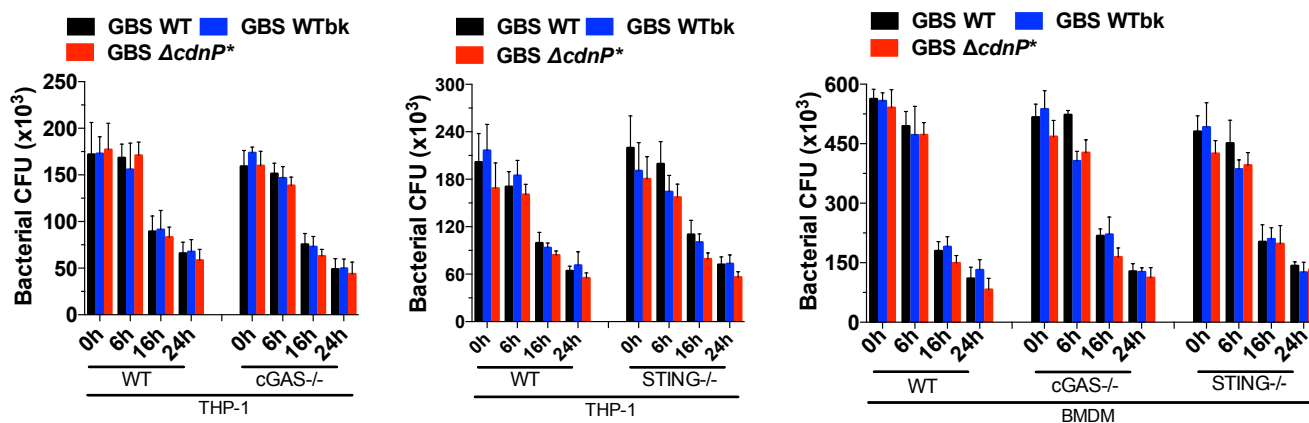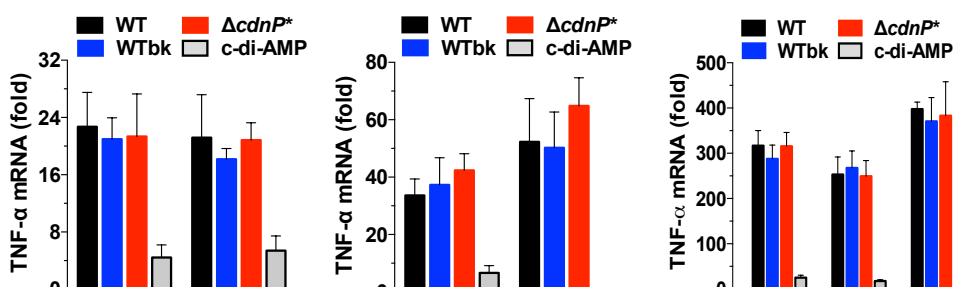
A **GBS *in vitro* growth rate**
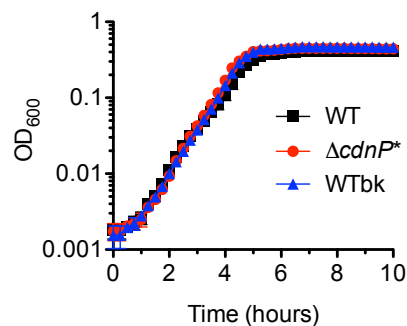
B **Phagocytosis**

C **Intracellular killing**

D **TNF-α induction**

Supplemental Figures

Figure S1 (Related to Figure 1).
STING expression in THP-1 CRISPR/Cas9 cells.
Whole lysates from WT and STING KO THP-1 cells were subjected to western blotting using antibodies against STING and β-actin.

Figure S2 (Related to Figures 2 and 4).
The Δ*cdnP** supernatant contains an increase amount of c-di-AMP.
(A) Representative chromatograms of GBS supernatant fractions containing c-di-AMP. Supernatants from overnight growth of the WT (black), the Δ*cdnP** mutant (red), and the WTbk control (purple) were filtered and fractioned on a C18 Sep-Pak column. Each fraction was analyzed by HPLC. c-di-AMP was exogenously added to the WT supernatants (blue line) and recombinant rCdnP was added to the Δ*cdnP** supernatants and incubated at 37°C for 1 hr (green line). Peaks corresponding to c-di-AMP are highlighted by dotted lines.
(B) Relative quantification of c-di-AMP in the WT (black) and the Δ*cdnP** mutant (red). Supernatants were incubated with the c-di-AMP binding protein CabP and, after washing and elution, c-di-AMP was quantified by HPLC.
(C) GBS supernatant fractions were incubated with digitonin-permeabilized WT and STING$^{-/-}$ THP-1 cells for 6 hrs. c-di-AMP (100 nM) was used as a positive control. Levels of IFN-β were normalized to GAPDH levels. Data are the mean +/- SD of at least two independent experiments.

Figure S3 (Related to Figure 3).
CdnP specific activities.
(A) Schematic representation of the two-step degradation of 2',3' cUMP into uridine by CdnP. The CdnP phosphodiesterase activity converts 2',3' cUMP into 2' or 3' UMP and the CdnP nucleotidase activity further hydrolyzes the remaining phosphodiester linkage to release inorganic phosphate and uridine. The CdnP specific activity on different cyclic nucleotides was quantified by following the release of P_i using malachite green after incubation of 3 nM rCdnP with 2mM of substrates in the presence of 2 mM Mn^{2+}. Samples were taken every 10 min and activities are expressed as μmol of P_i per min per mg of proteins.
(B) Schematic representation of the two-step degradation of c-di-AMP into adenosine by the sequential activity of the two CdnP and NudP ectonucleotidases. The CdnP phosphodiesterase activity cleaves c-di-AMP into two AMP molecules, which are further hydrolyzed into adenosine by the NudP 5' nucleotidase activity. The CdnP specific activity on different cyclic di-nucleotides was measured as in (A) in the presence of NudP.
(C) Chemical structure of cyclic diadenosine monophosphorodithioate, Rp-isomers (Rp, Rp-c-diAMPSS), a di-thiophosphate analogue of c-di-AMP and its inhibitory effect on c-di-AMP hydrolysis by CdnP. The kinetic of c-di-AMP hydrolysis was followed by RR-HPLC by measuring the quantity of AMP formed in the presence of 100 μM c-di-AMP and different concentrations of Rp, Rp-c-diAMPSS.

Figure S4 (Related to Figure 4).
Bacterial growth rate, phagocytosis, intracellular killing and TNF induction are not affected by CdnP inactivation.
(A) GBS *in vitro* growth curve. Overnight cultures of the WT (black), the Δ*cdnP** mutant (red), and the WTbk control (blue) were diluted 500 times in THB + 50 mM Hepes. Optical densities (OD$_{600}$) were monitored every 15 minutes in a micro plate reader at 37°C. Mean and S.D. were calculated from 4 independent overnight cultures and 8 technical replicates for each strain.
(B) Bacterial phagocytosis. GBS WT, WTbk, or the Δ*cdnP** mutant were used to infect THP-1 or BMDM and the corresponding cGAS and STING deficient cell lines at an MOI of 6 at the

indicated time points. Viable intracellular bacteria were quantified following cell lysis. Data are represented as mean ± SD of two independent experiments.

(C) Intracellular killing. GBS WT, WTbk, or Δ*cdnP** mutant were used to infect THP-1 or BMDM and the corresponding cGAS and STING deficient cell lines at an MOI of 6 for 2 hrs (corresponding to time 0). The kinetics of bacterial killing was followed for 24 hrs by enumerating viable intracellular bacteria after cell lysis. Data are represented as mean ± SD of two independent experiments.

(D) TNF induction. WT, cGAS^{-/-} and STING^{-/-} THP-1 cells were infected with GBS WT, WTbk, or Δ*cdnP** mutant (MOI-6) or transfected with c-di-AMP (100 nM) for 4 hr. Levels of TNF-α mRNA were determined by qPCR and normalized to GAPDH levels. Data are represented as mean ± SD of three experiments.

Supplementary Experimental Procedures

Bacterial strains and growth conditions

Todd Hewitt (TH, Difco-BD) agar or Columbia agar supplemented with 10 % horse blood (BioMerieux) was used for GBS isolation. Liquid cultures were done at 37°C in TH broth (THB) or in a chemically defined medium (CDM) containing 1 μM $FeSO_4$, $Fe(NO_3)^2$, 700 μM $MgSO_4$, 55 μM $MnSO_4$, 90μM $CaCl_2$, 0.2 μM p-aminobenzoic acid, 3.7 μM NAD, 4.1 μM pyridoxamine dihydrochloride, 0.07 μM Vitamin B12, 4.1 mM L-cysteine, 55 mM $NaC_2H_3O_2$, 29.7 mM $NaHCO_3$, 26.6 mM NaH_2PO_4, 51.7 mM Na_2HPO_4, 55 mM glucose, 0.2 mM each of adenine and uracil, and 0.1g/l of the 20 amino acids. *Escherichia coli* DH5 α (Invitrogen), BLi5 (Munier et al., 1992) and XL1 Blue (Stratagene) were grown in Luria-Bertani Broth (LB) medium. When specified, antibiotics were used at the following concentrations: for *E. coli*: erythromycin, 150 μg/ml; kanamycin, 30 μg/ml; chloramphenicol 30 μg/ml for GBS: erythromycin, 10 μg/ml.

Construction of the Δ*cdnP** GBS mutant

The predicted CdnP catalytic histidine residue at position 199 was substituted with an alanine by replacing the corresponding codon on the GBS chromosome. Site-directed mutagenesis by a splicing by overlap-extension method, GBS transformation, and mutant isolation were done as described (Heckman and Pease, 2007; Firon et al., 2013; Firon et al., 2014) Briefly, two PCR products with overlapping ends containing the $H_{199}A$ substitution were generated with primers 418 + 419 (TCAT<u>GATTC</u>ACAAGTGGTTTAGCTGTTCAAGC and GTAATCTAAACCGTAATTAAACTCtgcATTACCTAGTGTTGATGCATCA) and 420 + 421 (TGATGCATCAACACTAGGTAATgcaGAGTTTAATTACGGTTTAGATTAC and ACTA<u>GGATCC</u>TTTCCATTGATACCATCAACTCC), mixed together in a second PCR reaction with the external primers 418 + 421, and cloned between the *EcoR*I-*BamH*I sites of the pG1 thermo-sensitive shuttle plasmid containing the erythromycin resistance gene. Transformation of GBS with the pG1 Ω *cdnP** vector was done by electroporation and selected on erythromycin at 30°C (permissive temperature for pG1 replication). Chromosomal integration of the pG1 Ω *cdnP** vector at the *CdnP* locus was obtained in the presence of erythromycin at 37°C (non-permissive temperature). Excision of the integrated vector can give the expected $H_{199}A$ substitution (the Δ*cdnP** mutant) or can restore the wild type *cdnP* allele (corresponding to the isogenic WTbk control). The loss of pG1 was performed by serial dilutions at 30°C without antibiotic selection, followed by confirmation of erythromycin sensitivities at 37°C. After isolation at 37°C without antibiotic, analytic PCR was performed to differentiate the Δ*cdnP** clones and the WTbk controls with Δ*cdnP** specific primer pairs 422 + 423 (AGCGTATTCGCTTTAACTGTCTT and GTAATCTAAACCGTAATTAAACTCTGC) and

6

425 + 426 (TAGCACTACTTTCGGAGACTTGC and TGATGCATCAACACTAGGTAATGCA) and the WTbk specific primers pairs 422 + 424 (AGCGTATTCGCTTTAACTGTCTT and GTAATCTAAACCGTAATTAAACTCATG) and 425 + 427 (TAGCACTACTTTCGGAGACTTGC and TGATGCATCAACACTAGGTAATCAT). Sanger sequencing (GATC Biotech) was performed on 422 + 425 PCR products to confirm the mutated and the wild-type *cdnP* alleles in the corresponding strains.

Cell culture, and CRISPR/CAS9-Mediated Knockout Cell Line Generation

THP-1 cells (a human promonomyelocytic cell line) were grown in RPMI1640 supplemented with 4 mM glutamine and 10% fetal bovine serum (FBS). To generate targeted mutations, THP-1 cells were coelectroporated with a gRNA- and a mCherry-Cas9-expression plasmid as described (Schmid-Burgk et al., 2014). The gRNA target sequences used were GAACTTTCCCGCCTTAGGCAGGG for cGAS (Wassermann et al., 2015), TCCATCCATCCCGTGTCCCAGGG for STING, and CGGACACCTTACTCCCTTTG for IFI16. After FACS enrichment of mCherry-Cas9-positive cells, monoclones were grown for 2 weeks and were genotyped using deep sequencing. For each target gene, clones bearing all-allelic frameshift mutations were expanded for further study. Western blotting with cGAS, IFI16, STING and β-actin specific antibodies confirmed the absence of expression of the targeted protein. Primary BMDMs of WT, cGAS$^{-/-}$ and STING$^{-/-}$ mice were cultured in Dulbecco's modified Eagle's medium (DMEM; Gibco-BRL) supplemented with 4 mM glutamine and 10% FBS.

Cell infections

Cells were infected or stimulated as described (Charrel-Dennis et al., 2008). Briefly, after an overnight culture without agitation at 37°C in THB made with endotoxin-free water, GBS cultures were diluted in THB and grown to mid-logarithmic phase (OD650 = 0.5). After two washes in PBS, GBS was used to stimulate cells at an MOI of 6 (except when stated). After 3h, ciprofloxacin 10 μg/ml was added to limit the growth of residual extracellular bacteria. Cells were harvested 6 hrs post-infection for RNA preparation (except when stated) followed by mRNA quantification by qRT-PCR. For protein quantification, cell culture supernatants were analyzed 18 hrs post-infection by ELISA. Transient transfections with GBS DNA and c-di-AMP (Biolog Life Science GmbH) were performed with Lipofectamine 2000 (Invitrogen) according to the manufacturer's instructions.

Phagocytosis and killing assays

For phagocytosis and killing assays, WT and mutated THP-1 and BMDMs were infected with GBS strains and viable intracellular bacteria were quantified by plating serial dilution on plates. For phagocytosis assays, cells were infected for 1, 2 and 4 hrs with the different GBS strains (MOI 6), extensively washed to remove extracellular bacteria and cells were resuspended in 0.5% saponin in sterile antibiotic-free medium containing 10% heat-inactivated FBS and incubated for 5 min at 37°C, then vortexed thoroughly to permeate cell membranes. The lysed cell mixture was serially diluted in sterile medium containing 0.5% saponin and cultured on 5% sheep blood agar plates overnight (Remel; Lenexa, KS). For the killing assay, cells were infected for 2 hrs, washed to remove extracellular bacteria and cells were lysed with 0.5% saponin, serially diluted and cultured on 5% sheep blood agar plates (at t 0 of infection). After 6, 16 and 24 hrs, cells were washed to remove extracellular bacteria, lysed, and plated as described before.

Quantitative RT-PCR

Total RNA was extracted from infected cells using Trizol (Invitrogen) according to the manufacturer's instructions. One microgram of total RNA was used for cDNA synthesis using iScript Select cDNA Synthesis Kit (Bio-Rad), and quantitative PCR was performed using iQ SYBR Green Supermix (Bio-Rad). The following primers were used: human IFNβ forward AGGACA GGATGAACTTTGAC and reverse TGATAGACATTAGCCAGGAG; human TNFα forward TGCTTGTTCCTCAGCCTCTT and reverse GGTTTGCTACAACATGGGCT; human GAPDH forward GAGTCAACGGATTTGGTCGT and reverse TTGATTTTGGAGGGATCTCG; mouse IFNβ forward TCCGAGCAGAGATCTTCAGGAA and reverse TGCAACCACCACTCATTCTGAG; mouse TNF-α forward CAGTTCTATGGCCCAGACCCT and reverse CGGACTCCGCAAAGTCTAAG; mouse GAPDH forward CGACTTCAACAGCAACTCCCACTCTTCC and reverse TGGGTGGTCCAGGGTTTCTTACTCCTT.

Quantification of GBS intracellular cdN by LC-MS/MS

Extraction of cdNs was performed on 5 ml of overnight bacterial cultures. After washing, bacterial pellets were resuspended in 300 µl of extraction buffer (Acetonitrile/Methanol/Water, 2/2/1, v/v/v), incubated at 4°C for 15 min, and heated at 95°C for 10 min. After centrifuging (20,800 g, 10 min, 4°C), supernatants were collected and the extraction was repeated twice with 200 µl of extraction buffer without the heating step. The three supernatants were pooled and dried (speed-vac). Quantification of cdNs was performed by LC-MS/MS by Biolog Life Science GmbH using internally labeled standards. Protein quantifications (BCA) were performed on 5 ml of overnight cultures in parallel of cdN extraction. Quantities of cdNs were normalized to the protein concentration of prepared supernatant samples.

Quantification of cdN and nucleotides by RR-HPLC

Rapid Resolution High Performance Liquid Chromatography (RR-HPLC) using a reverse-phase column (Agilent ZORBAX Eclipse XDB-C18, 2.1 x 50 mm, 1.8 µm) was used to determine kinetics of extracellular c-di-AMP degradation on whole GBS cells, extracellular c-di-AMP quantification, and for CdnP enzymatic characterization. Samples were analyzed by RR-HPLC with a flow rate of 0.25 ml/min and a linear gradient of 1–12% CH_3CN (2–13% CH_3CN or 1-90% CH_3CN) in 20 mM triethylammonium acetate buffer, pH 7.5. Quantification was performed by comparing the peak areas of relevant cdN in the sample with those in standards of known concentrations.

Extracellular c-di-AMP degradation by GBS

Overnight cultures of GBS were diluted (1/100) and incubated at 37°C until they reached an $OD_{600} = 1$, corresponding to the early stationary phase. After centrifugation (10 min, 4,000 rpm) and washing, pellets were resuspended in Tris 50 mM, pH 7.5, supplemented with 5 mM $MnCl_2$ (corresponding to the optimal assay condition for CdnP enzymatic activity). The cells were incubated at 37°C with agitation and the reaction started by adding 0.1 mM c-di-AMP (Biolog Life Science GmbH). Aliquots were taken at different time points, centrifuged two times to eliminate bacteria, and kinetics of c-di-AMP degradation and product formation were quantitated by RR-HPLC by integrating the corresponding nucleotide peak areas using known nucleotide standards as controls.

Quantification of c-di-AMP in GBS supernatants

To analyze the level of extracellular c-di-AMP in supernatants, GBS strains were cultured at 37^oC in 50 mL of CDM media until late exponential growth phase ($A_{600} = 0.6$). Bacteria were eliminated by centrifugation (4,000 rpm, 10 min, 4°C) and the supernatant was subsequently

filtered through 0.2 µm nitrocellulose membrane filters (Millipore). Supernatants were then applied to Sep-Pak columns (Waters Corp., 6cc, 500 mg C_{18}) by gravity. The column was subsequently washed in succession with 5 x 1mL of water. Each wash was collected as a separate fraction, lyophilized and analyzed by RR-HPLC.

To quantify the levels of extracellular c-di-AMP, we included an affinity purification step using the c-di-AMP binding protein CabP from *S. pneumoniae* (Bai et al., 2014). This additional step was necessary given the high volume of supernatants to be treated and the low amount of c-di-AMP in wild-type GBS supernatants. The *cabP* gene was synthesized (Genscript), cloned into the pET28a expression vector (NdeI-HindIII), and propagated into the *E. coli* Bli5 strain in LB containing kanamycin and chloramphenicol. CabP expression was induced with 0.5 mM IPTG in exponentially growing cultures (A_{600} = 0.6). After 3 hrs of induction at 20°C, 100 ml of cultures were pelleted (4,000 rpm, 15 min, 4°C), washed with PBS and the pellets were resuspended in EWB (NaH_2PO_4/Na_2HPO_4 50mM, NaCl 300mM, [pH=7.0]). Cells were lysed with a French press at 14,000 p.s.i., and cell debris was eliminated by centrifugation (12,000 rpm, 20 min, 4°C). The His-Tagged CabP (estimated by UV and SDS-PAGE to be 2 mg for 100 ml of culture) was then fixed on TALON resin (0.75 ml) previously equilibrated in the same buffer for 20 min at 20°C. The His-Tagged CabP fixed on the resin was then centrifuged (700 g, 5 min, 4°C) and washed two times with PBS buffer before use.

Supernatants of GBS were passed successively through a 0.45 µM filter and a Vivaspin 3 kDa to remove most of the secreted proteins and small macromolecules. The CabP-containing resin was added to the filtered supernatant and incubated for 2 hrs at 4°C with agitation. As a control, 40 ml of PBS containing 1.25 µM c-di-AMP was used instead of supernatant and treated in the same condition. After the incubation, the CabP-containing resin was centrifuged (700 g, 5 min, 4°C), washed two times, resuspended in water and heated (95°C, 5 min). A final centrifugation step (14,000 rpm, 10 min) allows recuperating the supernatant containing the c-di-AMP bound to CabP and liberating by heating. After lyophilization, c-di-AMP was resuspended in 50 µl of 50 mM Tris and 1 µl was quantified by RR-HPLC as described previously. For IFN-ß induction assays, WT and STING^{-/-} THP-1 cells were stimulated with the CabP-purified supernatants with a supernatant/buffer ratio of 1:1 (40 mM Hepes [pH 7.2], 10 mM $MgCl_2$, 4 mM ATP, 4 mM GTP, 20 µg/ml digitonin) for 4 hr, as described (Zhang et al., 2014). Total RNA was extracted and RNA levels were measured by qPCR.

Cloning and purification of rCdnP

Recombinant CdnP (residues 29-768) was produced by first cloning a high fidelity PCR reaction (Phusion DNA polymerase, Thermo Scientific) obtained using GBS NEM316 genomic DNA as the template and primers gbs1929NcoI: (ATGCCCATGGAAGACATTGTTACAACACCAAGTTCAACCTC) and gbs1929Xho (AGCTCTCGAGTGTTTTTTCTTTCTGTTGTGTATAGACAGTGCC). The resulting NcoI-XhoI digestion product was cloned into the pET24d expression vector digested with the same restriction enzymes and gel purified. After Sanger sequencing (GATC Biotech), the resulting pET24dΩCdnP-His plasmid was transformed into *E. coli* BLi5 cells with kanamycin and chloramphenicol selections. Large-scale preparations of proteins were done on 650 mL of LB culture of *E. coli* BLi5 / pET24dΩCdnP-His. Briefly, an overnight culture was diluted (1/100), incubated at 30°C until the late exponential phase (A_{600} = 0.7), and expression of rCdnP was induced for 3 hrs by adding 1 mM IPTG. Cells were harvested (5,000 rpm, 10 min, 4°C) and frozen at -20°C. Cells were resuspended in 20 ml Tris, 300 mM NaCl, pH 7.0, and cells were disrupted by passaging through a French press at 14000 p.s.i. Cell debris was eliminated by centrifugation (12,000 rpm, 20 min, 4°C) and rCdnP-His was purified by chromatography on a 5 ml TALON crude column with a linear gradient from 0 to 150 mM Imidazole gradient in 50 mM Tris, 300 mM NaCl, pH 7.0, at 5 ml/min for 20 min. Fractions containing the enzyme were

pooled, concentrated on Vivaspin 20 kDa and purified on a Hi Load Superdex S200 column previously equilibrated with 50 mM Tris, 100 mM NaCl, pH 7.0, at a flow rate of 1 ml/min. SDS-PAGE electrophoresis and Coomassie Blue staining revealed a single protein (purity >98%) consistent with the predicted 80 kDa rCdnP-His molecular weight. Protein concentration was determined spectrophotometrically by UV absorption at 280nm using a ε_{280} = 76670.

Analytical Ultracentrifugation

Sedimentation velocity experiments were carried out at 20°C in an XL-I analytical ultracentrifuge (Beckman Coulter). Samples (1 mg/ml) were spun down using an An60Ti rotor and 12-mm double sector epoxy centerpieces at 42,000 rpm and interference profiles were recorded every 5 min. Data were processed with the Sednterp software to estimate the partial specific volume of CdnP (0.732 ml/g), and the buffer viscosity (1.027 centipoises) and density (1.0044 g/ml). Sedimentation coefficient distributions, $c(s)$, were determined using the software Sedfit 14.1. Sedimentation coefficients values are presented for standard conditions (in water at 20°C).

Enzymatic activity assays

To characterize the CdnP enzymatic parameters, its metallo-phosphatase activity was first assayed on 2',3' cyclic nucleotides by measuring the release of inorganic phosphate (P_i) using the Malachite Green reagent following the manufacturer's recommendations (*BIOMOL GREEN*[TM], Enzo Life Sciences). The reaction was performed with 3 nM purified rCdnP at 37°C in 50 mM Tris adjusted to different pHs (between 5.5 and 8.5) and containing various concentrations of cofactors (Mn^{2+}, Ca^{2+}, Mg^{2+}, Zn^{2+}, Co^{2+}) and 2 mM of 2',3' cNMP. After stopping the reaction with 1 ml of *BIOMOL GREEN*[TM] reagent, samples were incubated at room temperature (20-30 min) and inorganic phosphate (P_i) was quantified by spectrophotometric absorbance measurements at 620 nm against a standard P_i curves. Kinetics with cdN were done at 37°C in 50 mM Tris, pH 7.5, containing 5 mM $MnCl_2$, 100-200 µM of substrates, and 3 nM purified rCdnP enzyme. Substrate degradation and product formation were followed every 7 min by RR-HPLC. Sequential degradation of cdN into nucleosides was done in the same conditions in the presence of an excess amount (50-250 nM) of the second ectonucleotidase rNudP purified as described. Quantification of Pi resulting from the sequential degradation of cdN by CdnP and NudP was done using the Malachite Green reagent.

References Cited in Supplemental

Heckman, K.L., and Pease, L.R. (2007). Gene splicing and mutagenesis by PCR-driven overlap extension. Nat Protoc *2*, 924-932.
Munier, H., Bouhss, A., Krin, E., Danchin, A., Gilles, A.M., Glaser, P., and Barzu, O. (1992). The role of histidine 63 in the catalytic mechanism of *Bordetella pertussis* adenylate cyclase. J Biol Chem *267*, 9816-9820.
Schmid-Burgk, J.L., Schmidt, T., Gaidt, M.M., Pelka, K., Latz, E., Ebert, T.S., and Hornung, V. (2014). OutKnocker: a web tool for rapid and simple genotyping of designer nuclease edited cell lines. Genome Res *24*, 1719-1723.